07:27:06 OCA PAD AMENDMENT - PROJECT HEADER INFORMATION 06/25/92

Active

Project #: E-19-693 Cost share #: Rev #: 2
Center # : 10/24-6-R7018-1A0 Center shr #: OCA file #:
Work type : RES
Contract#: UNC 5-33646 Mod #: AMEND. 6/24/92 Document : AGR
Prime #: DHHS/NHLBI/ HL 42075-03 Contract entity: GTRC

Subprojects ? : N CFDA:
Main project #: PE #: N/A

Project unit: CHEM ENGR Unit code: 02.010.114
Project director(s):
YOGANATHAN A P CHEM ENGR (404)894-2849

Sponsor/division names: UNIV OF NORTH CAROLINA / CHAPEL HILL, NC
Sponsor/division codes: 400 / 080

Award period: 910701 to 930630 (performance) 930630 (reports)

Sponsor amount	New this change	Total to date
Contract value	0.00	57,405.00
Funded	0.00	57,405.00
Cost sharing amount		0.00

Does subcontracting plan apply ?: N

Title: CARDIOPULMONARY GEOMETRY & BLOOD FLOW IN GROWING LAMBS

PROJECT ADMINISTRATION DATA

OCA contact: Kathleen R. Ehlinger 894-4820

Sponsor technical contact

DR. CAROL L. LUCAS
(919)966-3411

U. OF NORTH CAROLINA AT CHAPEL HILL

Sponsor issuing office

SARAH W.THOMPSON,CONTRACT SPECIALIST
(919)962-5011

U. OF NORTH CAROLINA AT CHAPEL HILL
CAMPUS BOX 1350
440 W. FRANKLIN STREET
CHAPEL HILL, NC 27599-1350

Security class (U,C,S,TS) : U ONR resident rep. is ACO (Y/N): N
Defense priority rating : N/A N/A supplemental sheet
Equipment title vests with: Sponsor X GIT
PER ARTICLE XIII, P. 7
Administrative comments -
AMENDMENT SIGNED BY GTRC 6/24/92 EXTENDS BUDGET PERIOD THROUGH 6/30/93.

GEORGIA INSTITUTE OF TECHNOLOGY
OFFICE OF CONTRACT ADMINISTRATION

NOTICE OF PROJECT CLOSEOUT

SK100

Closeout Notice Date 09/28/93

Project No. E-19-693 Center No. 10/24-6-R7018-1A0

Project Director YOGANATHAN A P School/Lab CHEM ENGR

Sponsor UNIV OF NORTH CAROLINA/CHAPEL HILL, NC

Contract/Grant No. UNC 5-33646 Contract Entity GTRC

Prime Contract No. DHHS/NHLBI/ HL 42075-03

Title CARDIOPULMONARY GEOMETRY & BLOOD FLOW IN GROWING LAMBS

Effective Completion Date 930630 (Performance) 930630 (Reports)

Closeout Actions Required:	Y/N	Date Submitted
Final Invoice or Copy of Final Invoice	Y	930819
Final Report of Inventions and/or Subcontracts	Y	
Government Property Inventory & Related Certificate	N	
Classified Material Certificate	N	
Release and Assignment	N	
Other	N	

Comments EFFECTIVE DATE 7-1-91. CONTRACT VALUE $57,405.

Subproject Under Main Project No.

Continues Project No. E-19-656

Distribution Required:

Project Director	Y
Administrative Network Representative	Y
GTRI Accounting/Grants and Contracts	Y
Procurement/Supply Services	Y
Research Property Managment	Y
Research Security Services	N
Reports Coordinator (OCA)	Y
GTRC	Y
Project File	Y
Other CARL BAXTER-FMD	Y
FRED CAIN-OOD	Y

NOTE: Final Patent Questionnaire sent to PDPI.

RESEARCH PLAN

Introduction to Revised Application

The initial review group of this competing continuation proposal seemed enthusiastic about the major objective of the project--to improve current methodology for repairing congenital defects that impair blood flow to the pulmonary circulation. The aims were considered to be well focused and to address problems of substantial clinical relevance. However, major concerns were expressed in five areas:

1) the nature of progress in the current grant period, with specific criticisms directed at the quality of the flow visualization studies,

2) lack of methodological detail as to how the computational studies are to be performed,

3) the methods by which data from proposed new studies will be manipulated quantitatively, interpreted, and brought to bear on the clinical question,

4) failure to take into account the compliance of the pulmonary system,

5) inability to determine which phase of the cardiac cycle is represented by the methyl methacrylate cast and resultant flow-through models.

This revised application addresses these concerns by:

1) updating and expanding the progress report while defending the quality and scientific appropriateness of the flow visualization work,

2) adding substantial detail to the Methods Section describing the finite element implementation and techniques to be used to calculate shear stress, flow separation and reattachment, energy losses, etc.,

3) expanding a concluding portion to the Methods Section (under Consolidation Aim) outlining information to be gained from studies performed under each of the Specific Aims experimental protocols--*in vivo, in situ, in vitro,* and *computational* studies--and how they are related to each other and the clinical problem at hand,

4) incorporating studies in compliant structures when feasible, while maintaining our position that compliance is relatively unimportant in proposed studies in which flow conditions will be relatively nonpulsatile and the extracardiac conduits under investigation will be relatively noncompliant,

5) acknowledging that the casting technique, in which casts are obtained from deceased animals whose vascular beds have been perfused with saline before being dried with nitrogen, does not enable determination of the phase of the cardiac cycle under consideration.

Specific actions taken in each of these areas of concern are described in more detail below:

1) **Progress in the current grant period:** At the time of the competing renewal, the only studies completed with sufficient data to warrant journal publication were in the area of flow visualization. The method employed by the Fluid Dynamics Laboratory at Georgia Tech for presenting these findings--videotaping the process, capturing frames from the videotape on a computer, following the movement of particles from frame to frame, and then assimilating those findings via computer-assisted/hand-rendered streamlines--is still considered state-of-the-art, as can be observed by examining mainstream journals in the field, e.g., *Journal of Biomechanics, Microcirculation,* and *Journal of Biomechanical Engineering,* in which the flow visualization work has just been accepted for publication. A copy of the paper is in submitted as an Appendix. To enable direct visualization of the raw data, an audioless videotape was submitted with the previous application. To assist the viewer in assimilating and interpreting the findings, an audio track has been added to that tape for this revision. (Appendix 1)

Other additions to the progress report include updates on the status of a) *in vivo* work including a table of equations (Table 1, page 39) for calculating age-dependent physiologic parameters b) *in situ* work including the 3D framework developed for referencing branching angles and generating an age-dependent, mathematical formulation of the pulmonary outflow tract and bifurcation area that can be used in computational studies to project growth (Table 2, page 45), c) an update on the status of *in vitro* pulsed Doppler ultrasound studies, and d) statements indicating the time intensive nature of the data collection portions of some studies (not including data analysis), e.g., 5 days/*in vitro* pulsed Doppler ultrasound study, 3 months/*in vitro* laser Doppler study, 3 weeks/cast preparation for CT scanning, 20 hours computer time/conversion from the CT taped 2D images of each cast to the 3D volume rendered image, etc.

We believe that the additions to the progress report clearly demonstrate the importance of the research completed during the initial phase of this project. The combined *in vivo*, *in situ*, and *in vitro* approach provides a unique global picture of age-related changes in the geometry and physiologic parameters of the normally maturing lamb pulmonary artery--from the outflow tract through the bifurcation area. The equations in Tables 1 and 2 provide information needed to derive a wealth of information. For example, steps demonstrating a possible sequence for estimating main pulmonary artery (MPA) compliance/distensibility in a 42 day old lamb are:

From Table 1--mean MPA pressure=13.1 mmHg, systolic MPA pressure = 20.4 mmHg, diastolic MPA pressure=8.6 mmHg, pressure-strain elastic modulus (Ep)=102 mmHg

From Table 2--diameter of MPA at valve=1.82 cm, diameter of MPA at bifurcation=1.51 cm, length of MPA=6.21 cm

Intermediate computations--ΔP=systolic-diastolic pressure=11.8 mmHg, D_a=average diameter = 1.66cm, A_a=area at D_a=2.17cm^2, V_a=volume assuming uniform tube=A_a•length=13.48cm^3, diameter at systole=(systolic pressure-mean pressure)/Ep=1.78cm, diameter at diastole=(mean pressure-diastolic pressure)/Ep=1.59cm, ΔD=.19cm, area at systole=2.49 cm^2, area at diastole=1.98cm^2, ΔA=0.51cm^2, $\Delta V=\Delta A$•length (assuming fixed/tethered length)=3.16cm^3.

Compliance estimates--$C=\Delta V/\Delta P$=0.267cm^3/mmHg=0.000201cm^5/dyne, distensibility=$K=(\Delta V/V)/\Delta P$=0.0199/mmHg=0.0000149cm^2/dyne, $100\bullet\Delta D/D_a$=11%, $100\bullet\Delta A/A_a=100\Delta V/V_a$=23%, etc., with the % values agreeing closely with those reported for normal human MPAs *in vivo* using MRI techniques.[1] (More precise estimates could be found by integrating the above sequence appropriately along the length of the tapered vessel.)

In addition, a mathematical model of the geometry, including projected curvatures and branching angles could be visualized in 3D on a computer screen, and, with the addition of values for heart rate (143 bpm), pulmonary vascular resistance (259 dyne-s/cm5), and cardiac output (2.15L/min), velocity profiles could be simulated *in vitro* (current technology in noncompliant tubes) and computationally (work in progress).

The nature of the approach taken is such that major publications involving the *in vivo* and *in situ* work are best formulated after all the animal work is completed, i.e. when complete data sets are available over all age ranges studied. With the exception of the need for additional animals in older age groups (6 months and 1 year), *in vivo* studies are complete. (Animals earmarked/purchased at birth for these studies are just reaching the appropriate age.)

2) Methodology: The Methods Section was expanded to more fully describe the finite element approach we are taking for computational fluid mechanics studies. The hardware (Cray Y-MP) and software (FIDAP) selected are those supported by the recently opened (Spring 1990) North Carolina Supercomputer Center. Key features of the simulation process are the external geometry/surface defining mesh, the internal computational mesh, the boundary conditions, the solution, and meaningful ways to visualize results. Since our primary goal is to examine the effects of geometry on solutions, we have focused efforts on methods for efficiently developing and manipulating geometry meshes between our computer and the supercomputer. Upstream (velocity profiles) and downstream (pressures) boundary conditions will we consistent with our *in vivo* findings. FIDAP is a powerful package possessing most of the capabilities needed for simulations in

3D once the meshes and boundary conditions are defined. The ability to move 3D surface boundaries (within FIDAP) as a result of pressure changes is projected to be available within the calendar near.

3) **Elaboration of how data from proposed new studies are to be manipulated quantitatively, interpreted, and then brought to bear on the clinical question at hand:** The "CONSOLIDATION AIM" material added at the end of the Methods Section is organized to present a concise overview of the manner in which intra- and interstudy (*in vivo, in situ, in vitro,* and *computational*) data are to be manipulated and integrated. The manner in which the results obtained will be used to answer basic questions related to interactions between geometry and fluid dynamics is summarized for each basic question posed. The manner in which the answers to these basic questions will have an impact on needed answers to several important clinical problems is likewise summarized for each problem posed.

4) **Compliance of the cardiopulmonary system:** The normal pulmonary arterial bed is undoubtedly more compliant than the systemic vascular bed, a factor that greatly influences features such as pressure and velocity waveform shapes, input impedance spectra configurations, and right ventricular work. Based on results obtained in our investigation of the relationship between age and MPA compliance in growing lambs, compliance can and will be incorporated into the computational studies. As indicated above, we are in the process of implementing a technique that combines the velocity-pressure solutions generated by FIDAP with surface boundaries independently by determined pressure-diameter relationships.

   Incorporating compliance into *in vitro* work is challenging. Models that enable comparable flow visualization, pulsed Doppler ultrasound, and laser Doppler anemometry (LDA) studies must be made of transparent, synthetic materials. None are currently available that accurately mimic the compliance properties of biological tissue. To date, given available equipment at Georgia Institute of Technology, laser Doppler work had to be performed in flow-through configurations embedded in acrylic blocks. As indicated in the previous submission, work by other investigators has indicated that compliance is not a major determinant of the flow fields in large vessels.

   The recent acquisition of the Dantec 3D fiberoptic LDA system via an NIH large equipment grant will enable us to measure velocity in compliant structures. This has been demonstrated by recent studies in Japan by Professor Hayeshi and colleagues,[2] who used a similar LDA system to measure velocities in an *in vitro* compliant model of the descending aorta. For the studies proposed, however, the importance of incorporating this factor is even less apparent than it was for the studies pertaining to normal flow patterns. The primary configurations to be investigated are atrio- and cavopulmonary connections and extracardiac shunts in which pulsatility will be determined by the pattern of venous return plus what little pulsatility may be imposed by right atrial contraction. Ultrasound Doppler and MRI measurements indicate that venous blood flow into the right atrium is relatively nonpulsatile.[3] Thus the flow approaches steady state, which significantly diminishes the importance of compliance as a relevant parameter. The extracardiac shunt configurations themselves will consist of homographic and/or synthetic materials that are also relatively rigid and noncompliant.

5) **Cardiac Cycle Phase Determination for Casts:** No marked improvements can be made given the current resources of our laboratories, which do not have CT or MRI facilities available for studies in animals. When the investigation moves to humans and/or such facilities become available to us for animal work, information gained from medical imaging modalities can be used for flow model reconstructions as well as computational studies. Our best indication of the relative validity of the current technique is that the measured MPA diameters of the completed cast approximate average external diameters measured in vivo within a range of 5-10%. Given that casts represent internal diameters and that methyl methacrylate has a shrinkage rate of 2-5%, these measurements are very encouraging. Current techniques available for casting the entire right ventricle and the pulmonary arteries are relatively lengthy, and therefore cannot be done at a fixed phase in the cardiac cycle. We are not attempting to cast a short segment of a vessel.

Added sections are indicated by solid vertical lines at the margins. Paragraphs with substantive changes are indicated by dashed lines at the margins. The abstract was shortened to meet the size criteria of the 9/91 PHS 398 forms. Several figures in the original application were eliminated.

1. SPECIFIC AIMS

The long-term objective of this proposal is to determine relationships between cardiopulmonary geometry and pulmonary blood flow patterns in growing lambs. The goals of the current phase are 1) to establish the effects of normal growth and development on the geometry of the right ventricle and major pulmonary arteries and 2) to evaluate relationships between the geometric configurations observed and the resultant pulmonary fluid dynamics. The goals of the proposed phase are 1) to evaluate the fluid dynamics associated with surgical repair options for congenital defects interrupting or severely impairing the pulmonary circulation--to examine perioperative results and to project the impact of growth on those results, and 2) to develop computational techniques that facilitate evaluation of surgical materials and procedures--to provide a computer aided design (CAD) tool for previewing repair options. We hypothesize that the proposed studies will help identify causes of graft failure and will assist cardiologists and surgeons in selecting the optimal timing for interventions that establish optimal pulmonary blood flow patterns and make appropriate allowances for patient growth. Specific aims are:

Aim 1: In Vivo Studies

a. To obtain pressure and velocity (pulsed Doppler ultrasound) profiles in the main and branch pulmonary arteries and relevant inflow regions of lambs before and after performing surgical procedures associated with improving pulmonary blood flow in congenital lesions (e.g., pulmonary and tricuspid atresia and tetralogy of Fallot). Interventions to be considered include: implantation of extracardiac conduits (homografts and synthetic conduits) and modifications of the Fontan procedure.
b. To evaluate the importance of right atrial contractions to pulmonary blood flow. To examine pressure and flow characteristics under conditions of normal and abnormal atrioventricular conduction.

Aim 2: In Situ Studies

a. To obtain silicone rubber casts from the animals studied *in vivo* that clearly display geometric features of the right heart, inferior and superior vena cava connections, and major pulmonary arteries.
b. To provide valved homografts for *in vitro* studies by harvesting pulmonary arteries and aortas and associated valves from animals first studied for other purposes.

Aim 3: In Vitro Studies

a. To perform flow visualization and pressure mapping studies in mock-ups of right heart-pulmonary artery connections. Available methyl methacrylate casts will provide the geometry of the right heart and pulmonary arteries of lambs ranging in age from 1 day to 1 year. Conduits will be made from commercially available materials and harvested homografts. Effects of conduit size and design will be tested in a range of hemodynamic conditions 1) keeping the geometry fixed and varying the conduit and 2) keeping the conduit fixed and varying the geometry to simulate expected growth and development. Detailed analyses will be made of energy losses caused by bends, kinks, etc. and factors affecting blood flow distribution to right and left lungs.
b. To perform flow visualization and pressure mapping studies in sub- and supra-valvular pulmonary stenosis. Existing flow-through models will be modified to simulate clinical stenotic patterns.
c. To perform flow visualization and pressure mapping studies in anatomically exact flow-through models made by encasing the silicone rubber casts obtained *in situ* in a clear liquid polymer.
d. To perform velocity profile studies within the flow-through models using pulsed Doppler techniques similar to those used in the *in vivo* studies.
e. To conduct laser Doppler anemometry studies in selected models to obtain more detailed 3D velocity profiles with better spatial resolution and to measure wall shear stresses.

Aim 4: Computational Studies

a. To expand the technique developed for quantifying the structure of the pulmonary outflow tract and main bifurcation as revealed by 3D reconstructions of CT scans of the casts made *in situ*. Additional generations of the pulmonary vascular tree and the entire right heart will be added to the analyses. Computer algorithms will measure key geometric features of the structures.
b. To develop finite element techniques for simulating pulmonary blood flow in normal and abnormal geometries. Structural boundaries needed to generate meshes for the simulations will be obtained from the reconstructed 2D and 3D images of the CT scanned casts. Once results in original geometries are validated, results expected from modifications will be projected.

Aim 5: Consolidation. To unify results obtained from the *in vivo, in situ, in vitro* and *computational* studies.

2. BACKGROUND AND SIGNIFICANCE

THE CLINICAL PROBLEM: Congenital heart defects, which result from deviations in the developmental process programmed to transform a simple straight tube into a complex four-chamber heart with separate pulmonary and systemic circulations,[4] are present in approximately 8 per 1000 live births.[5] Many of these defects interrupt or severely impair the right heart-pulmonary artery blood flow pathway via pulmonary and/or tricuspid stenosis or atresia--as isolated lesions or features of other lesions such as tetralogy of Fallot. Prior to the development of surgical shunt procedures connecting systemic to pulmonary arteries (e.g., Blalock-Taussig in 1945 [6] and Potts in 1946 [7]), patient survival depended on the presence of coexisting defects, e.g., a patent ductus arteriosus and a septal defect, that likewise enabled shunting of blood from the systemic to the pulmonary circulation. Surgical shunts were palliative and were not a solution leading to a normal life span.[8] For patients with pulmonary atresia, early repair procedures effecting a separation of pulmonary and systemic pathways included reconstruction of the pulmonary outflow tract with a synthetic extracardiac conduit (Rastelli et al. in 1965 [9]) or an aortic valved homograft (Ross and Somerville in 1966 [10]). In 1971, Fontan and Baudet [11] successfully implemented an atriopulmonary connection in a patient with tricuspid atresia, and the "Fontan" procedure or one of its many modifications is still the repair option of choice in patients who qualify, i.e., those who have reasonable anatomy of the caval veins, normal pulmonary vascular resistance, etc.

"Modified Fontan" has become a generic term applied to various procedures involving construction of atrioventricular (pulmonary outflow tract with normal valve), cavopulmonary (bidirectional Glenn procedure), or atriopulmonary connections. Some of these connections require patches and/or extracardiac conduits. Early dissatisfaction with homografts--postoperative calcification in frozen, irradiated grafts and problems in availability of fresh grafts--led to development of synthetic (Dacron) conduits containing bioprosthetic porcine valves, which were used extensively in the 1970s.[12] Reports of long term results for these conduits are mixed, with patency rates reported between 75-80% at one year and 0 to 50% at 10 years.[13] Attempts at angioplasty are generally unsuccessful. Late conduit obstruction usually develops secondary to pseudointimal peel formation in the wall of the conduit.[8,12,14-19] The site of obstruction occurs most often at the anastomosis or at the site of the valve, with the valve being involved in 40-60% of the cases. In addition to obstruction, primary causes of conduit failure are valvular stenosis and the patient outgrowing the conduit.[12]

The above findings suggest that, at least for conduits in the low pressure atrio- and cavopulmonary connections, valves may be neither needed nor desired.[20] The need for the right atrial contractions once thought necessary to impel the blood through an atriopulmonary connection is being questioned as a result of successful cavopulmonary connections that bypass the right atrial chamber under the hypothesis that maximum energy is conserved when connections are straight, i.e., intervening chambers or bends should be eliminated whenever possible.[21] Recent success with fresh and cryopreserved homografts suggests that graft material is one key to conduit success.[13] Though development of the cryopreservation technique has markedly increased the availability of homografts, the design flexibility inherent in synthetic conduits, plus the need at times to augment homografts with synthetic materials, makes continued research in this area desirable. Investigators are currently considering different prosthetic materials (e.g., polytetrafluoroethylene) and modifications of Dacron designs (e.g., knitted or loosely woven preclotted and albumin-impregnated grafts or combinations of loosely woven inner layers to promote anchoring and tightly woven outer layers to prevent bleeding).[13, 22-25] Observations in our own operating room experience indicate that the angle of graft anastomoses is important in achieving flow distribution to both lungs.

In summary, success of surgical interventions to improve pulmonary blood flow in infants with congenital heart defects that impede flow to the pulmonary circulation depends on the timing of surgical interventions, the procedures and materials selected, and the ability of the intervention to accommodate for patient growth. Repair attempts often include creation of atrio- or cavopulmonary connections with or without extracardiac conduits. However, conduits don't grow, optimal designs for atrio- and cavopulmonary connections are controversial, and late results from clinical and autopsy studies show high incidences of conduit failure. Thus, in spite of significant surgical advances, answers are still needed to many important questions, such as: *1) how to prevent conduit failure? 2) how to maintain sufficient energy to move blood through a low pressure system? 3) how to*

optimally distribute flow to both lungs--considering bulk flow as well as velocity patterns? and 4) how to anticipate and prepare for reasonable growth?

CONTRIBUTIONS TO BE MADE BY THIS PROPOSAL. Answers to the general questions above depend on answers to more specific questions regarding basic relationships between fluid mechanics and the involved geometries: *1) how do conduit design and shape effect shear stresses, secondary flow and flow separation? 2) how do curves, kinks, pouches, bends, etc., effect pressure/energy losses? and 3) how do anastomotic geometries (size, angle, relative placements and compliances, etc.) influence flow distribution to a parallel system?* Obtaining answers to these basic questions is the goal of this proposal.

The goals of the current (initial) phase of this project were to answer two questions relative to normal growth and development of the cardiopulmonary system: *1) how do the geometric configurations of the right ventricle and major pulmonary arteries change from birth to adult life? and 2) how do geometric variations as a result of normal aging and/or individual variability affect flow dynamics?* Based on results obtained in our laboratory and studies reported in the literature, we hypothesized that large-vessel geometry plays as important a role as hemodynamics in determining velocity patterns.[26-27] Obviously, vessels increase in size, but changes in curvature and/or branching angles were expected to be more important features relative to fluid dynamics. The impetus of these initial studies under normal aging conditions, and for the studies being proposed, is improving diagnosis and care of infants and children with impaired pulmonary circulations. To interpret clinical data accurately, the effects of a rapidly growing and changing geometry must be delineated from the effects of abnormal hemodynamics.

Though many of the analyses for this initial phase are incomplete, results obtained to date already provide a valuable data base from which to launch a detailed investigation of the fluid mechanics and growth potential of surgical options for establishing/improving right heart-pulmonary artery continuity: 1) methyl methacrylate and silicone rubber casts of hearts of lambs varying in age from 1 day to 6 months are available as models for mock-ups of intra- and extracardiac connections; 2) techniques have been developed for entering the geometry of the casts into computer storage and using 2- and 3-dimensional reconstructions of those data to measure key features and to provide boundaries for meshes for computational fluid dynamic studies; 3) facilities are in place for performing sophisticated *in vitro* studies under hemodynamic conditions consistent with pediatric as well as adult patients; 4) our hypothesis that geometric features, particularly curvature, play an important role in determining flow characteristics has been confirmed, [28-29, Appendices 2 and 3] a factor that must play a critical role in successful conduit design.

Reports abound in the literature of patient outcomes after surgical corrections for congenital heart defects [13,30] and the fate of intra- or extracardiac shunts placed in relatively large dogs;[20,24,31-34] however, comparable reports related to smaller/younger animals and/or lambs are limited. As part of this proposal, a limited number of *in vivo* studies are planned in which selected modifications of the Fontan procedure will be implemented in small (1 month old) and large (3 months old) lambs. Pulmonary hemodynamic studies, including pressure mappings, branch artery blood flow distribution, velocity profile studies, and color flow mapping, will be performed before the intervention, after the intervention, and during manipulations thought to simulate existing conditions in patients likely to undergo these procedures. Results obtained, including silicone rubber casts of all the pertinent geometry, will bring the problems under consideration into the "pediatric" arena and will provide a basis for establishing realistic "Fontan" flow patterns for *in vitro* studies.

Continued development of sophisticated techniques for visualizing flow and measuring point velocities in anatomically realistic models of vascular sections emphasizes that much still needs to be learned about relationships between geometry and cardiovascular fluid dynamics.[35-45] The predilection of regions of vessel branchings and curvature to develop atherosclerotic plaques is well known.[46-48] Evidence is mounting that geometric variations that lower hemodynamic shear at aortic and carotid bifurcations should be considered risk factors as important as family history and serum cholesterol level. Friedman and co-workers [49-50] have identified four geometric features of aortic bifurcations that lower shear stress at particular sites on the vessel wall: 1) a large angle of one or both daughters with the aortic axis, 2) a flow divider that does not lie on the axis of the terminal aorta, 3) an arterial branch that makes a large angle with the aortic axis while the other branch

closely follows that axis, and 4) a gentle intrusion of the arterial wall into the flow as the flow divider is approached.

We hypothesize that such geometric features--branching angles, wall intrusions, etc.--play key roles in successful conduit implantations, i.e., features known to promote atherosclerosis could reasonably be expected to promote pseudointimal peel formation. Surgical interventions creating anastomosis between structures not previously connected, particularly when synthetic materials are used, have potential for even more pronounced geometrical and mechanical mismatches--compliance mismatches, size mismatches, suture lines, attachment angle and size, etc.[23] Improving material characteristics will not in itself solve all conduit failure problems, for existing materials consistently work well in some areas and not in others that would appear to have similar biocompatibility requirements. For example, conduit failure is more prevalent in right-sided than in comparable left-sided applications.

In vitro studies provide flexibility not available *in vivo*; flow patterns can be observed under conditions of 1) constant hemodynamics and cardiopulmonary geometry and variable conduit designs (shape, size, anastomotic geometry, material, etc.), 2) constant hemodynamics and conduit design and a "growing" cardiopulmonary geometry, and 3) constant cardiopulmonary and conduit geometry and variable hemodynamics. While extensive work has been performed in curved tubes and in bifurcation and bypass models with various branching angles and curvature, with the exception of our laboratories, little has been done using this approach for examining the right-sided circulation. Yoganathan and co-workers have studied a rigid, planar model of the main, right and left pulmonary arteries of an idealized "normal" adult human, incorporating physiologically realistic branching angles and dimensions to determine the effects of stenotic pulmonic valves as well as sub- and suprapulmonic stenosis on fluid dynamics.[51-57] DeLeval [21] and co-workers used simple models to demonstrate the benefits of using cavopulmonary rather than atriopulmonary connections by showing that pressure energy is lost when flow passes through chambers or turns and when flow is pulsatile rather than continuous. We propose to expand these studies using more realistic models of infant cardiopulmonary geometry obtained via this project, adding the variations described above.

Just as *in vitro* studies provide flexibility not possible in *in vivo* studies, *computational* studies provide flexibility not practical in *in vitro* studies, theoretically umlimiting the number of hemodynamic and geometric variations that can be examined. Ideally, images obtained from MRI, CT, or even echocardiographic technologies would be used to generate 3-dimensional reconstructions of the patient's heart and relevant vessels, a technology already realizable [58-60]. The fluid mechanics of repair options could be previewed and needed prosthetic devices custom made prior to surgery, saving intraoperative time. CAD (computer aided design) tools are not new to surgery,[61-62] but computational fluid mechanics capabilities would add an exciting new dimension for approaching cardiovascular problems in general, and congential heart disease problems in particular. The proposed studies take the first step in this direction.

IMPORTANCE OF COLLABORATION. The studies proposed expand the project in directions consistent with the collaborating laboratories' major research interests and areas of expertise: 1) diagnosis and treatment of infants and children with congenital heart disease (The University of North Carolina Pediatric Cardiology and Cardiothoracic Surgery Research Laboratory) and 2) fluid mechanics of the heart and major vessels (The Georgia Tech Cardiovascular Fluid Mechanics Laboratory). The combined attack--1) *in vivo* studies in realistic animal models, 2) *in situ* casting of relevant structures, 3) *in vitro* studies combining state-of-the-art flow visualization, laser Doppler anemometry and pulsed Doppler instrumentation, and 4) *computational* studies with long term potential for providing a CAD tool for clinicians deliberating between repair options--will provide a comprehensive picture of fluid mechanics of current surgical interventions for establishing/improving pulmonary blood flow in a variety of congenital lesions. The collaboration developed for this project has been productive and rewarding on many levels, and we believe this will be demonstrated in the progress report that follows.

3. PROGRESS REPORT / PRELIMINARY STUDIES

I. PERIOD COVERED BY THIS REPORT:
This is the first Competing Continuation application for the project.
Beginning Date for Report = July 1, 1989; Ending Date = May 31, 1992.

II. KEY PERSONNEL at University of North Carolina (UNC) and Georgia Institute of Technology (GT)
CL Lucas, PhD, Professor of Surgery and Biomedical Engineering, UNC,
DOB 02/13/40, SS# 504-50-2631, 50% effort-July 1989 to June 1990, 33% effort-July 1990 to date.
GW Henry, MD, Chief of Pediatric Cardiology and Associate Professor of Pediatrics,
DOB 06/04/51, SS# 238-76-7875, 25% effort-July 1989 to date.
BR Wilcox, MD, Chief of Cardiothoracic Surgery and Professor of Surgery, UNC,
DOB 05/26/32, SS# 238-42-3563, Consultant, July 1989 to date.
AP Yoganathan, PhD, Professor of Chemical and Mechanical Engineering, GT,
DOB 12/06/51, SS# 569-27-7875, 25% effort-July 1989 to date.
M Singh, PhD, Visiting Professor of Surgery, UNC, from The Indian Institute of Technology, Madras,
DOB 05/11/42, SS# 246-90-1919, 25% effort-Sept 1989-June 1990, 100% effort July-August 1990.
JI Ferreiro, BS, Research Analyst I and Laboratory Director, UNC,
DOB 05/17/42, SS# 240-70-1502, 35% effort-July 1989 to date.
B Ha, PhD, Graduate Student Research Assistant/Postdoctoral Assoc., UNC,
DOB 09/09/62, SS# 414-33-8932, 100% effort-June 1989 to Dec 1989, 50% effort-Dec 1989 to date.
H Katayama, MD, Pediatric Cardiology Postdoctoral Assoc., UNC,
DOB 11/24/57, SS# 246-65-9623, 50% effort-March 1990 to date.
R Krzeski, MD, PhD, Burroughs Wellcome Fellow, UNC,
DOB 12/25/61, SS# 246-59-4869, 20% effort-July 1990 to date.
C Zhao, MS, Graduate Student Research Assistant, UNC,
DOB 04/11/60, SS# 222-72-0167, 50% effort-July 1989 to date.
R Zalesak, MS, Graduate Student Research Assistant, UNC,
DOB 07/11/52, SS# 455-84-1507, 50% effort-July 1989 to date.
H Demby, Graduate Student Research Assistant (NIH Predoctoral Minority Supplement), UNC,
DOB 08/23/58, SS# 245-06-4771, 50% effort-Jan 1991 to date.
H Sung, PhD, Postdoctoral Fellow, GT,
DOB 02/18/58, SS# 255-45-7679, 25% effort-July 1989-Feb 1990
E Muralidharan, Postdoctoral Fellow, GT,
DOB 05/09/59, SS# 260-75-3075, 25% effort-October 1990 to Dec 1991
Y Kim, Postdoctoral Fellow, GT
DOB 01/19/60, SS# 484-11-4483, 25% effort-Jan 1992 to date.
P Lynch, Graduate Student Research Assistant, GT,
DOB 03/26/65, SS# 214-92-0407, 100% effort-July 1989 to date.

III. SUMMARY OF SPECIFIC AIMS FOR CURRENT GRANT PERIOD
The major goals of the current grant period are 1) to determine the effects of normal growth and development on the geometry of the right ventricle and major pulmonary arteries and 2) to evaluate relationships between geometric configurations observed and pulmonary fluid dynamics. Specific aims are summarized as:

1. *In Vivo* Studies
   a. To obtain velocity profiles in the main (MPA, across long and short axes), right (RPA) and left (LPA) pulmonary arteries of normal lambs ranging from 1 day to 1 year in age using extraluminal and intraluminal pulsed Doppler probes.
   b. To obtain estimates of normal age-related changes in MPA compliance and pulmonary input impedance based on the velocity measurements obtained and simultaneously measured PA pressures and dimensions of major and minor axes.

2. *In Situ* Studies (capturing geometry)
   a. To obtain a series of resinous casts from the animals previously studied *in vivo* that clearly displays geometric features of the lumen of the right ventricle and major PAs of normally maturing lambs.
   b. To develop a technique for committing the structure of the casts as revealed by CT scans to computer memory, from which 2- and 3-dimensional images can be reconstructed for any desired plane or viewpoint and key geometric features can be determined.
3. *In Vitro* Studies
   a. To perform flow visualization studies--dye injections and laser light scattering--in glass flow-through models made from representative casts selected from each age group.
   b. To perform velocity profile studies within the glass models using pulsed Doppler techniques similar to those used in the *in vivo* studies.
   c. To perform laser Doppler anemometry velocity profile studies in selected models.
   d. To evaluate the relative importance of compliance versus geometry in determining pulmonary fluid dynamics.
4. Consolidation. To unify results obtained from the *in vivo*, *in situ* and *in vitro* studies and prepare a video presentation.

OVERVIEW: At the time of the writing of this report, significant progress has been made toward achieving all of the specific aims. *In vivo* studies have been performed on schedule; studies in seven of the nine age groups are relatively complete, and studies in the two age groups remaining are underway. For completed age groups, methyl methacrylate casts have been successfully obtained *in situ* and CT scanned. More animals than anticipated have been needed to complete studies in the younger/smaller age groups due to difficulty in performing hemodynamic studies and obtaining good casts in the same animal, i.e., due to concern that sutures used to close insertion points of the intraluminal pulsed Doppler needle probe would distort natural vessel shape. The computer process designed to quantitate cardiopulmonary geometry from the CT data for individual animals is operational, and a mechanism for formulating a "representative" structure for each age group is in place. *In vitro* studies have been completed in selected models, with some flow visualization results having been accepted for publication and Doppler results are being analyzed. To date, results obtained in *in vivo* and *in vitro* studies have been consistent, but further analyses are needed. A video presentation of our animated 3D velocity profile work and flow visualization work in glass and anatomically exact flow-through models is being included as part of this proposal. (Appendix 1)

IN VIVO HEMODYNAMIC STUDIES: The goal of this series of studies is to characterize normal age-related changes in pulmonary hemodynamic variables, including features of pressure and velocity waveforms, large vessel compliance (as indicated by pressure/diameter relationships) and afterload (as indicated by input impedance spectra). The first observation made was that "normal" lambs, like "normal" people, show considerable variability at all ages. Due to limited lamb availability, particularly in the summer and fall, we could not be as selective as originally planned. For example, the seven 1 month old lambs studied ranged in weight from 7.2 to 16.4 kgs with a mean weight of 12.2 kgs. However, we have been able to obtain a global, quantitative picture of changes to be anticipated. Data are still needed for larger animals, but the time constant of most parameters is such that 95% of the change occurs within the first three months (three time constants).

Hemodynamic Variables: Regression equations of the form $Y = A + B\, e^{-age/\tau}$, with age given in days, appear to be appropriate to describe most relationships observed. A table of equations and graphs of data and regression lines for PA pressures (Fig 1) and heart rate (Fig 2) are included below. Results are as anticipated, e.g., with maturation comes an increase in cardiac output accompanied by decreases in mean and systolic pressures, resistance, and heart rate. No age dependency between diastolic PA or left atrial pressures was found.

Velocity Profile Analysis: Recent efforts directed towards more detailed analysis of 2D velocity data [63-64] have yielded interpolated images such as those shown in Fig 3. The magnitude of velocities is presented by the color scale on the far right, where light blue indicates areas of marked negative velocities, pink-to-orange indicates areas of low or zero flow, and light yellow indicates areas of highest velocities. Data are shown for one cardiac cycle. The X axis represents time and the Y axis represents the distance from the posterior (left fig) or left wall (right fig) along a centerline axis. This technique clearly shows the timing of events along

TABLE 1. Physiologic Variables					
Mean MPA pressure (mmHg)	=	12.8	+	9.6	$e^{-age/12}$
Systolic MPA pressure (mmHg)	=	20.4	+	66.9	$e^{-age/5}$
Diastolic MPA pressure (mmHg)	=	8.6			
Mean Left Atrial pressure (mmHg)	=	3.0			
Mean central MPA velocity (cm/sec)	=	23	+	29	$e^{-age/6}$
Mean central RPA velocity (cm/sec)	=	19	+	22	$e^{-age/6}$
Max RPA velocity (cm/sec)	=	60	+	105	$e^{-age/9}$
Mean central LPA velocity (cm/sec)	=	18	+	22	$e^{-age/10}$
Max LPA velocity (cm/sec)	=	64	+	66	$e^{-age/9}$
Cardiac Output (L/min)	=	2.45	-	1.63	$e^{-age/25}$
Pulmonary Vascular Resistance PVR (dyne-sec/cm^5)	=	259	+	918	$e^{-age/5}$
Pressure-strain elastic modulus Ep(mmHg)	=	96	+	653	$e^{-age/9}$
Heart rate(/min)	=	62	+	137	$e^{-age/80}$

Fig 1. Age vs. PA Pressures

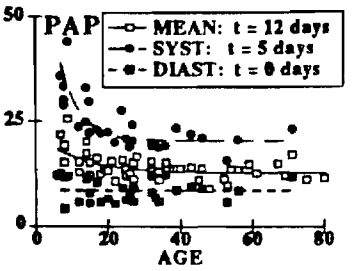

Fig 2. Age vs. Heart Rate

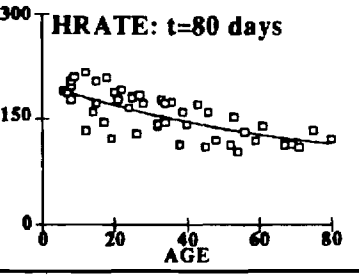

the axes: forward flow occurs earliest but has the shortest duration at the posterior wall. At the end of systole, represented by the black line drawn through the box, flow has already receded at the posterior wall but remains elevated at the anterior wall. Patterns along the right-left axis are relatively uniform across the vessel. The observations resulting from this analysis are consistent with those obtained from *in vitro* flow studies described below. Other visualization techniques are illustrated in Figs 10 and 17 and Appendix 4.

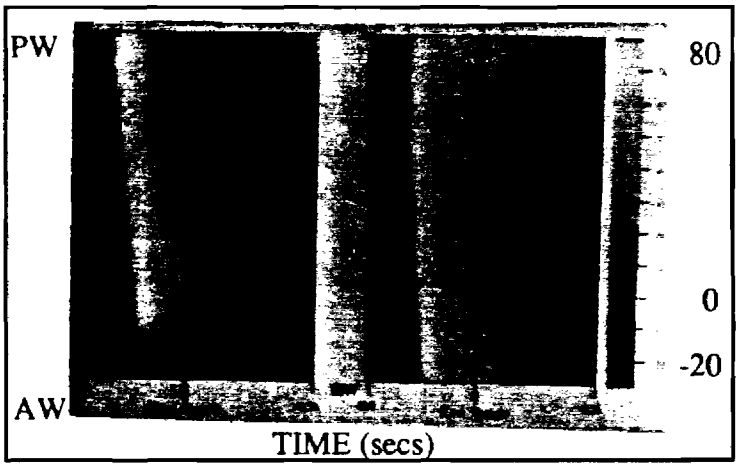

Fig 3. X Axis = Time, Y Axis=Location. See text for details

Compliance: Main pulmonary artery compliance and distensibility increase rapidly after birth. Up to a seven fold increase in compliance (estimated as $\Delta A/\Delta P$) can be observed in the first month. (Fig 4). This increase can be attributed to changes in wall properties in addition to rapid growth. Pressure-strain elastic moduli values ($Ep=\Delta P.R/\Delta R$), which in effect normalize for size, show an exponential decrease from approximately 400 mmHg at 1 week to 100 mmHg at 1 month (Fig 5). Results are similar along both axes, and a pooled Ep value was included in the Table above.

Fig 4. Pressure/Area Loops

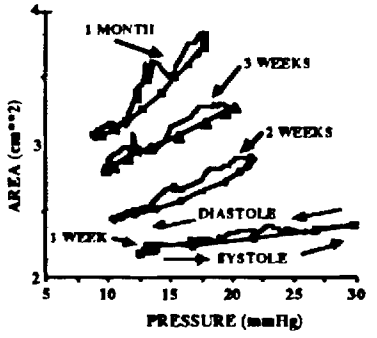

Fig 5. Age vs. Pressure-Strain Elastic Moduli

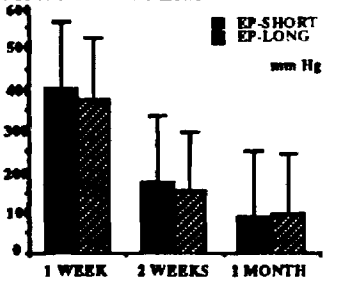

Input Impedance: Pulmonary input impedance to the main PA falls into the adult pattern rapidly, with the frequency of the first modulus minimum shifting from over 18 Hz to less than 10 Hz by the end of the first week-10 days. Results for ages 2 days, 1 week, 2 weeks and 1 month (Fig 6A) have been submitted for publication. Using estimates of propagation velocity, the shift in the modulus minimum was attributed to a shift in the primary reflection site. Input impedance spectra to right and left branches follow the same general time course (Fig 6B-C), with little change observed after the second week. These branch spectra will serve as guidelines for developing realistic downstream loads for *computational* studies.

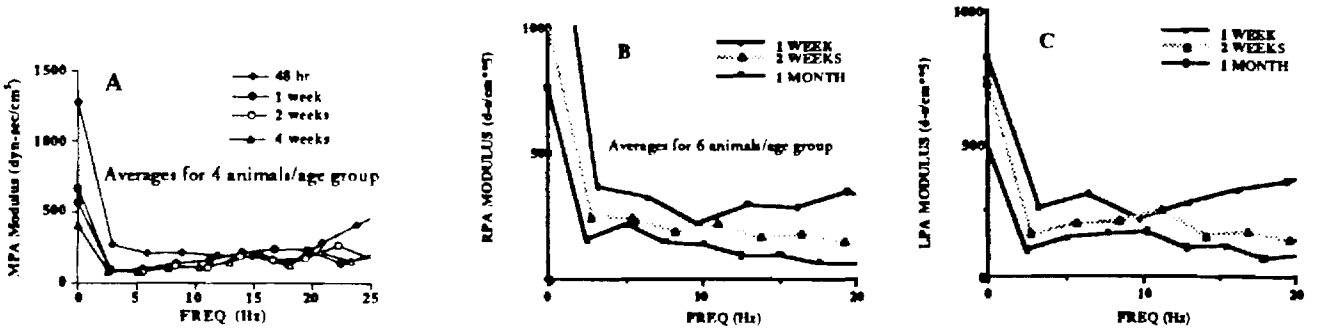

Fig 6. Input impedance spectra in main (A), right (B), and left (C) pulmonary arteries at ages specified.

IN VITRO STUDIES: The goal of this series of studies is to obtain quantitative measurements and insights regarding relationships between pulmonary geometry and physiologic conditions impossible to obtain *in vivo*, using flow visualization (FV) to define the global flow fields, pulsed Doppler ultrasound (PDU) to obtain quantitative measurements comparable to those obtained *in vivo*, and laser Doppler anemometry (LDA) to examine selected models and locations in depth. Given the time consuming nature of PDU and LDA studies, FV studies are performed first to select models to be considered for PDU studies, and both FV and PDU studies help guide the LDA studies. Time/study in one model under one set of physiologic conditions: FV = 1 day, PDU = 5 days, and LDA = 3 months.

IN SITU CASTING: In addition to the methyl methacrylate casts initially proposed for these studies, from which glass models are approximated at sizes large enough to be studied via laser anemometry, a method for developing completely anatomically accurate flow-through models--transparent acrylic molds of the right ventricular outflow tract and main and branch pulmonary arteries--has been implemented in the UNC-CH lab. Flow visualization studies have been performed in molds obtained for lambs weighing 2.4, 7.8, 9.5 and 11.5 kg. Vortex formation and retrograde flow appear to increase with flow rate as well as animal size. The results of this study have been published [29,65,66] and are submitted as Appendix 2.

Eleven glass models have been fabricated: original casts to scale (4 at ages 2 days, 2 weeks, 1 month, and 6 months), double scales of smaller original casts (2), variations in radius of curvature for 1 month old model (2), and variations in branching angle for 1 month old model (3).

FV: We have completed pulsatile flow visualization experiments on the three 1 month old models with varying radii of curvature: ∞ for straight tube, 80 mm for original cast, and 52 mm for exaggerated curvature.[57] These experiments were conducted at cardiac outputs (CO) of 3.5, 2.5 and 1.5 L/min (with corresponding pulmonary pressures of 30, 20 and 10 mmHg) and at heart rates of 70, 100 and 140 beats/min. The experiments were conducted using both white and laser light in the posterior/anterior and right/left planes. A blood analog fluid of 55% saline and 45% glycerine by weight was used with neutrally buoyant Amberlite particles. This work is in press [28] and has been submitted as an appendix (Appendix 3); however, general findings and representative figures from the study are summarized here.

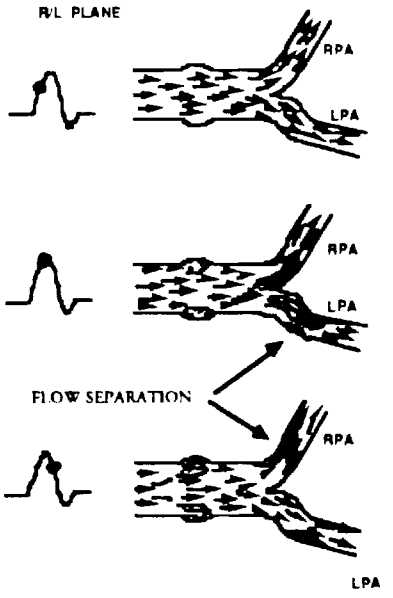

Fig 7. General flow fields.

Flow phenomena that were common to all three models were separation in the posterior sinus, separation regions along both the posterior and anterior walls in both the right and left pulmonary arteries, with prominent secondary

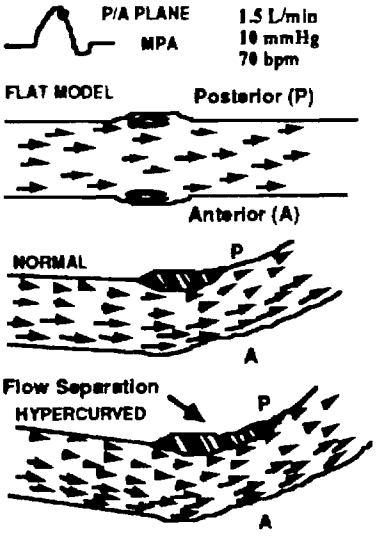

Fig 8. Flow reversal in MPA.

flow along the posterior wall of the RPA (Fig 7). Reverse flow in the curved models started along the posterior wall. As curvature increased, the flow in the vessel became much more disturbed and radial in nature and the separation regions grew larger and appeared earlier in the cycle (Fig 8). Comparisons of the pulmonary flow fields under varying heart rates revealed that flow separation regions appeared earlier in the cardiac cycle and developed faster at higher heart rates, but the size of the separation region decreased, as can be observed in the streakline photos included below (Fig 9). Comparisons of the pulmonary flow fields under varying pressure conditions (15 mmHg vs. 30 mmHg) revealed that as pressure increased, reverse flow increased in the distal portion of the MPA and in both daughter branches and fewer coherent structures, such as well defined vortices, were formed.

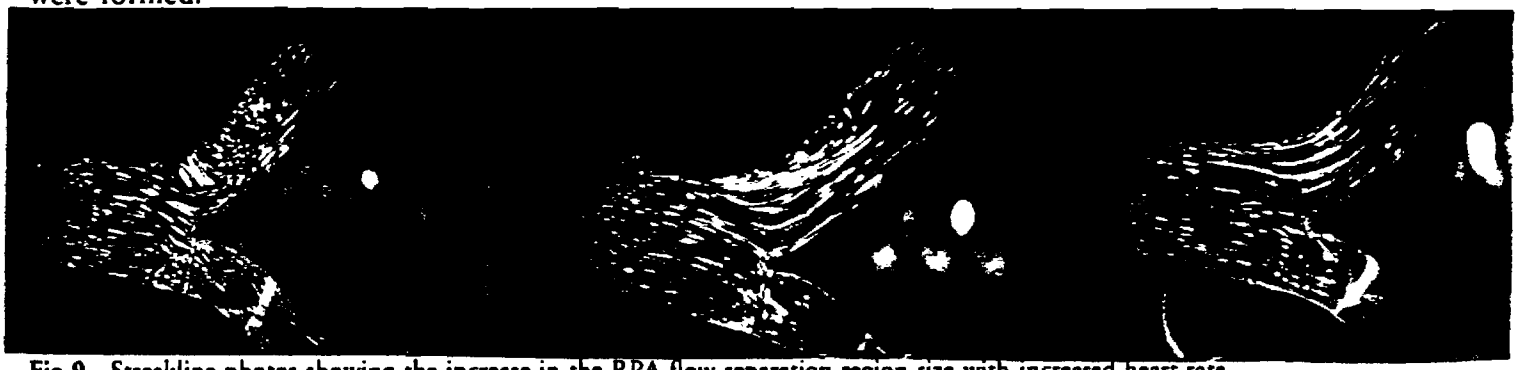

Fig 9. Streakline photos showing the increase in the RPA flow separation region size with increased heart rate. Left--70 bpm, Middle--100 bpm, Right--140 bpm.

The observed *in vitro* flow fields correlate well with those obtained in the *in vivo* studies: flow reversal in the main PA begins along the posterior wall, flow reversal is more pronounced in right than in left pulmonary arteries, and flow in the main pulmonary artery tends to be skewed toward the right wall. The studies clearly show that both geometry and physiology affect the pulmonary artery flow field. The size, location and appearance of flow separation regions are influenced by both the curvature of the main pulmonary artery and heart rate. The initiation of flow reversal is influenced by heart rate, while its magnitude is affected by the mean pulmonary artery pressure. The secondary and radial nature of the flow field is affected by curvature, heart rate, and mean pulmonary artery pressure. The observed dependence of the pulmonary flow field on both geometric and physiologic parameters, and the ability to isolate the individual contributions of these parameters on the pulmonary flow field through *in vitro* experimentation, further illustrate the important contributions to be made to our understanding of pulmonary flow fields through *in vitro* studies.

PDU: PDU studies have been completed and analyzed in the above models under one set of physiologic conditions: CO = 3.5 L/min, MPA pressure = 30 mmHg, and heart rate = 70 beats/min. Experiments for a second set of physiologic conditions--CO=1.5L/min, MPA pressure=10 mmHg, and heart rate=140 beats/min, have just been completed. A 2 mm diameter 10 MHz needle probe was used to measure the velocities in the main, right and left pulmonary arteries. The probe was inserted into the glass models of all three branches in both the plane of the bifurcation (the right to left plane) and the perpendicular (posterior/anterior) plane. In the main branch, axial measuring points were located 18, 21, 25, and 30 mm upstream from the bifurcation apex. Velocities in branches were measured in four locations downstream from the apex (3, 8, 12 and 17 mm for right branch, 4, 9, 15, and 20 mm for left). The probe was positioned so that the ultrasound pulses were oriented 0 degrees to the flow. Sequential velocity measurements were obtained by manually traversing the crystal in 2 mm increments across the vessel. In the perpendicular plane, the needle was traversed from the posterior wall to the anterior wall in all three branches. In the plane of the bifurcation, measurements were made from the right to the left wall in the MPA, and from the inner to the outer walls in the branches. At each sampling site (168 sites/model), the signals were recorded for 30 seconds using a Vingmed SD 100.

In comparing the velocity profiles, the most obvious effect of increasing curvature of the right ventricular outflow tract (RVOT) and the MPA is the concentration of flow reversal along the posterior wall in the MPA. (Fig 10A). In the flat model, reverse flow is concentrated in the central portion of the vessel. In the most highly curved model, flow reversal starts earliest, lasts longest, and reaches the highest negative velocity along the posterior wall. For example, in the 70 bpm study, flow reversal along the posterior wall begins 300 msec after the onset of systole, lasts for 112 msec, and has a maximum velocity of .14 m/sec. Along the anterior

wall, the fluid does not begin reversing until 336 msec into the cardiac cycle, lasts for only 60 msec, and reaches a velocity of only .06 m/sec. At peak systole, the velocity profiles in the curved models are skewed towards the posterior wall (Fig 10B). Flows in the left and right branches of all three models also show dependence upon RVOT and MPA curvature. While the profile in the right/left plane of all three models in the left branch is skewed toward the inner wall, as the model becomes more curved, the velocity profiles become M-shaped, indicating the presence of secondary flow (Fig 10C). As curvature of the model increases, secondary flow in the RPA increases, but the duration of flow reversal is less.

The PDU studies quantitatively verify the observations made in FV and in *in vivo* studies, and as do the FV

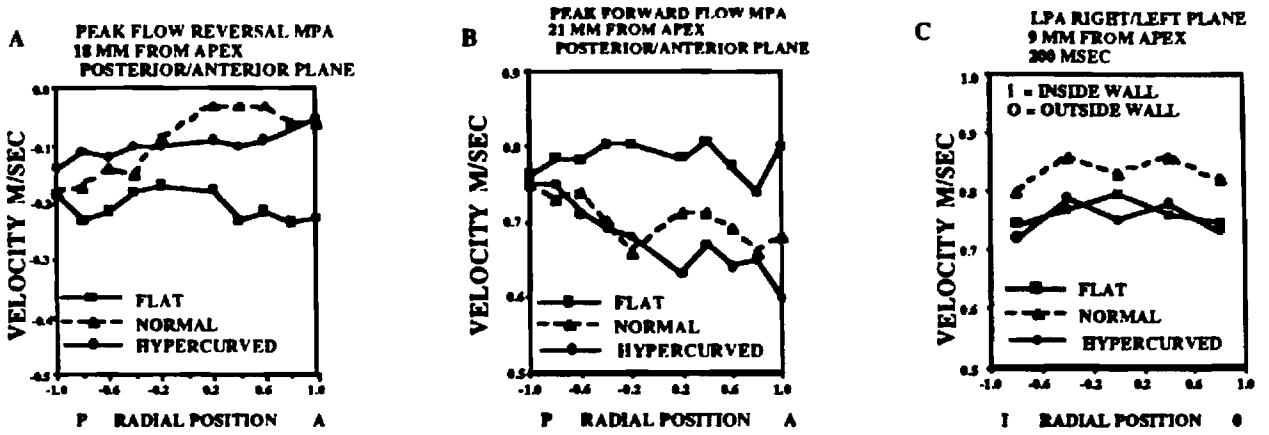

Fig 10. Selected velocity profiles from PDU studies: A--peak flow reversal in MPA, B--peak forward flow in MPA, C--forward flow pattern in LPA.

studies, highlight the importance of understanding the interaction between geometry and physiology. For example, the ability to measure flow reversal in models in which only the curvature varies clearly shows that the curvature has its primary effect on the distribution of flow reversal. The magnitude of peak flow reversal actually had an unexpected decrease with curvature. Thus the increase in flow reversal observed with increased pressure may be obscured by changes in curvature, a finding with important clinical implications.

LDA : LDA studies are being conducted during the current year of the project.

Importance of Compliance: Recent findings that vessel compliance has negligible influence on the bulk flow field have led us to delete the previously proposed compliance studies. Friedman,[67,68] Liepsch,[69-70] and Anayiotos [71] all studied the effects of arterial elasticity on blood flow in the human aorta and carotid arteries. These studies revealed that while increasing vessel compliance caused substantial alterations in near wall regions—i.e., a reduction of wall shear stress and decreased flow reversal—the effect on the bulk flow field was inconsequential. The applicability of these results to the more compliant pulmonary system may be questioned. A study by Wells et al. [72] found the vessel diameter changes of the adult human pulmonary arteries to be 4% greater than those of the descending aorta. Our study, however is focused on the pulmonary hemodynamics in newborn. While physiologic changes soon after birth cause a rapid increase in pulmonary vessel compliance,[73] the compliance is still less than that found in mature animals.

Equally important, the accuracy with which an *in vitro* study can ultimately mimic the elasticity of the natural vessel is itself questionable. Arterial walls are complex living structures with varying composition.[71] *In vitro* arterial models are frequently constructed with uniform wall thickness and compliance. No transparent synthetic materials are available that accurately mimic the complex compliance properties of biological tissues. For the *in vitro* FV and LDA studies, the models must be made from optically transparent material. The natural vessel is often considered to be a perfect cylinder connected to a pair of rigid ends. In reality, arterial vessel walls exhibit viscoelastic properties, and their movement is often hampered by surrounding organs and physiologic structures that produce a tethering effect.[71] Such tethering defines certain important geometric characteristics of the vessel such as curvature. A rigid *in vitro* model can more realistically reproduce the curvature of the RVOT and MPA than a compliant model. In such a situation, reproducing the curvature has a more profound effect (i.e., first order) on the flow field than the compliance (which is a second order effect).

FV at UNC: Given our interest in studying fluid dynamics in anatomically exact flow-through models that are often too small for laser Doppler work and an anticipated marked increase in *in vitro* studies, efforts have been made to establish some flow-visualization capabilities at the University of North Carolina (UNC) site. The laser light scattering technique used at Georgia Tech (GT) has been implemented at UNC, and results obtained from studies performed in four anatomically exact models under conditions of pulsatile flow have been reported above. To visualize streamlines in steady flow, a technique that appears particularly appropriate for studying the relatively nonpulsatile fluid mechanics experienced through the atriopulmonary connections, a rig has been constructed that greatly facilitates a systematic 3D approach to streamline visualization. The apparatus, designed by Dr. Singh, a visiting professor from IIT, Madras, India, is simple but elegant, and has been used in studies to examine fluid flow in curved tubes and at arterial bifurcations. [74-76] (Appendix 5)

Support for pilot studies of fluid dynamics in extracardiac shunts has been obtained from the North Carolina Heart Association (Belinda Ha, PI). Basic flow characteristics in shunt designs will be examined before incorporating the shunts into mock-up models including the right heart and pulmonary tree. A schematic of the first model has been fabricated. The tube is straight and includes an aperture for insertion of a mechanical pulmonary valve (Medtronic-Hall). The conduit is designed to include the ridges present in Dacron shunts. Additional models with varying degrees of curvature and internal wall characteristics will be studied in the first series of experiments.

QUANTITATION OF CARDIOPULMONARY GEOMETRY: The goal of this series of studies is to parametrically characterize the pulmonary artery outflow tract and bifurcation structure in three-dimensional space and to relate those parameters to age. Parameter sets must be complete, i.e., provide sufficient information to independently reconstruct a mathematical model of the original tree. By changing the parameters based on the age-dependent relationships, the tree can then be made to "grow." The model geometry can be exported for computational fluid dynamic studies. Each stage of the process is illustrated below: data entry, feature extraction, model reconstruction, and relationships between parameters and age. Thirty sets of data have been processed. Time requirements/cast are: preparation = 3 weeks, importing CT scan data into computer = 2 hours, processing imported CT data = 20 hours, and calculating geometric parameters = 2 hours. Results have been presented as posters at FASEB meetings. [77-78]

Data Entry: Computerized reconstructions of the images obtained from the CT scanned casts are being performed on a Stardent 3000 Graphics minisupercomputer. The steps to enter the 2D images into computer storage are performed with software (licensed name =USR/IMAGE) made available to us by the Medical Imaging Group associated with the Computer Science, Radiology and Biomedical Engineering Departments. Volume rendering (interpolation to transform the 2D images taken at 1.5 mm intervals into a 3D image) is accomplished using the Application Visualization System (AVS) computer software package. The structures of most interest--portion of outflow tract, main PA and proximal sections of branch PAs--are "segmented" from the image. The 2D-3D-segmentation process is illustrated in Fig 11.

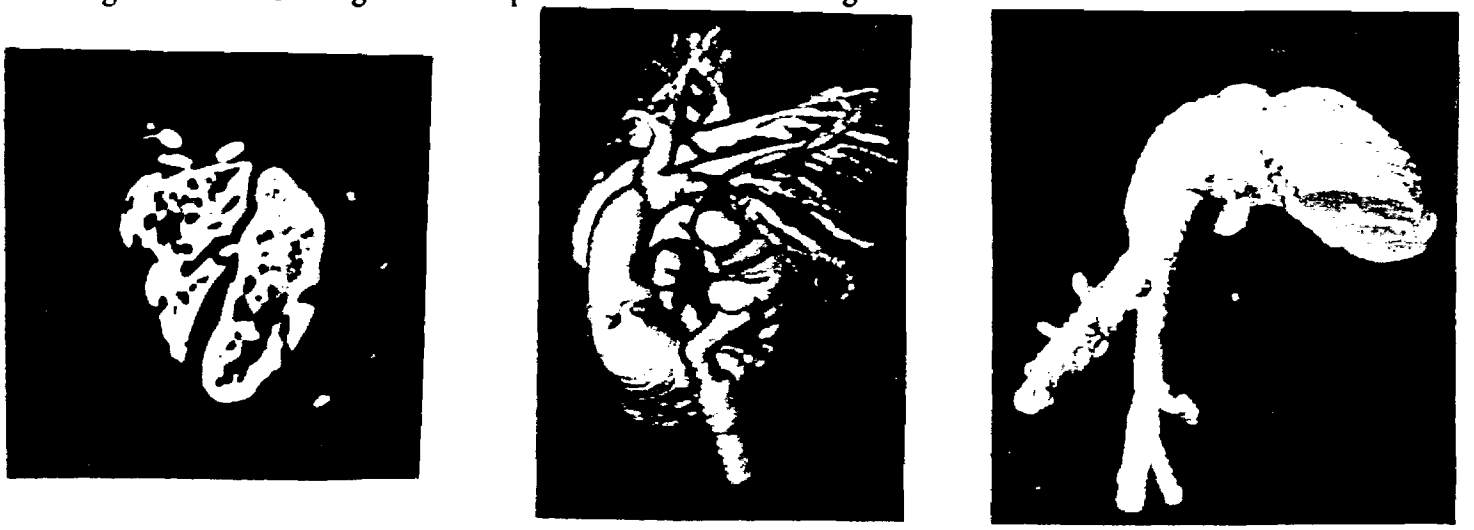

Fig 11. Left --CT Scan Slice, Middle--Volume Rendered Image, Right--Segmented PA Outflow Tract

Feature Extraction: A "thinning" method is applied to the segmented image to estimate points on the medial curves. A three-dimensional cubic spline is used to smooth the data and obtain medial curve functions--tangents, normals, etc. (Fig 12). The cross section of a vessel at a point is obtained by examining the intersection of the vessel walls with a slice plane whose normal is the derivative of the medial curve function at that point. Sequential cross-sections are used to construct a diameter profile beginning at a position on either the right or left pulmonary arteries and following up through the valve into the outflow tract. Distance is measured in terms of arc length along the medial curve. "Bumps" in the curve serve as landmarks for the bifurcation and valve areas. Taper (ΔDiameter/ΔLength) is calculated by curve fitting to the diameter profile between points of interest.

The medial curves of the 4 sections--the outflow tract, MPA, RPA, and LPA--are approximated by arcs. A 3D reference system is established from the intrinsic geometric features of the structure.(Fig 12) The three orthogonal axes of the reference system are the tangent of the MPA arc at the bifurcation junction point, the normal to the main arc plane, and the cross product (binormal) of these two vectors, respectively. The origin is located at the bifurcation junction point. All parameters are calculated using this reference system. Each section is fully described by a 6 parameter set. The set can be presented in several equivalent, transformable forms. A particularly descriptive set for the age-dependent analyses is: vertical angle from the origin, horizontal angle from the origin, radius or curvature, length, taper, and diameter at one end. The extrapolated curve for the MPA is used to estimate the branching angle between the MPA and each of the branches.

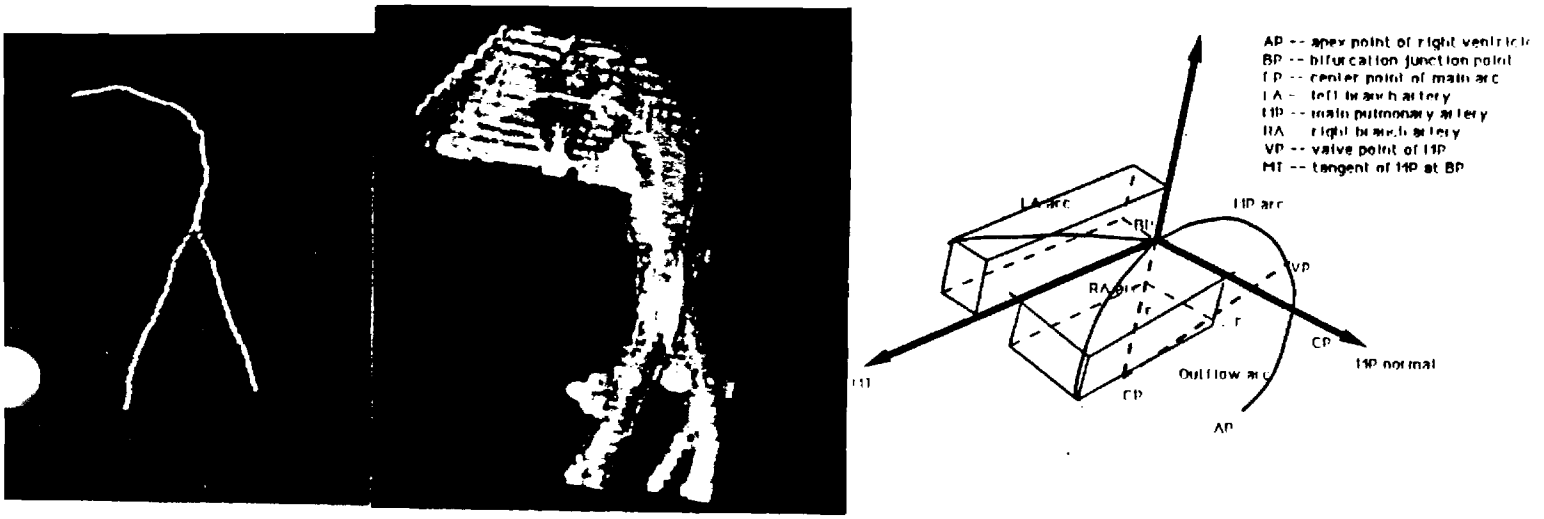

Fig 12. Left--Medial Curve obtained by thinning process. Middle--Volume superimposed over medial curve. Right--Intrinsic Reference System for Bifurcation Structure.

Mathematical Reconstruction: A scheme was devised by which segments could be constructed independently and then joined by matching corresponding nodes in the bifurcation areas. The basic unit is an octagon. At the bifurcation, each branch is connected to the other two branches by four consecutive points of the octagon, leaving a small triangular gap at the two three-vessel intersections. Away from the bifurcation, the octagonal surface points lie on cross-sectional planes that are normal to the medial arc. The segments can be visualized separately and transported "in pieces" to the finite element program. One model reconstruction is demonstrated below (Fig 13): the mesh as segments, the assembled mesh, the mesh volume rendered, and the original structure.

Fig 13. Left-to-Right: Individual segments of model, Model assembled, Model volume rendered, Original 3D construction

Geometry vs Age: As for *in vivo* variables, regression equations of the form $Y = A + B\ e^{-age/\tau}$ are appropriate to describe most relationships between parameters and age. Though interanimal variability is large, particularly in the branching angles of the younger age groups, the findings obtained yield valuable information about the growth patterns of lamb pulmonary arteries. Two such findings are:

1) the radius of curvature tends to increase with age for the RPA but decrease with age for the LPA (Fig 14)
2) taper decreases with age for the MPA and its branches, i.e., the diameter of the distal end of each vessel grows more rapidly than the diameter of the proximal end. The difference is so marked that if one considers the cross-sectional area ratios of the bifurcation to be the area of proximal branches/area of distal MPA (bifurcation end), the ratios are greater than one at birth and decrease to approximately .95. However, using the area of the proximal MPA (valve end), the ratio appears to increase slightly with age (Fig 15).

Based on measurements taken both *in vivo* and *in situ*, vessels are assumed to be circular in shape. Eccentricities at most positions are >.9, and no consistent diverging pattern has been found.

TABLE 2. Relationships between model parameters and age, subject to revision as older animal data are added, are:

Diameter of MPA at valve(mm)	=	22.7	-	10.5	$e^{-age/50}$
Diameter of MPA at bifurcation(mm)	=	18.4	-	9.0	$e^{-age/42}$
Diameter of RPA at bifurcation(mm)	=	12.5	-	5.4	$e^{-age/37}$
Diameter of LPA at bifurcation(mm)	=	11.6	-	4.6	$e^{-age/47}$
Length of MPA (mm)	=	69	-	30	$e^{-age/29}$
Taper of MPA	=	.051	+	.030	$e^{-age/12}$
Taper of RPA	=	.040	+	1.83	$e^{-age/1}$
Taper of LPA	=	.025	+	.191	$e^{-age/3}$
Horizontal angle RPA (degrees)	=	32	+	30	$e^{-age/2}$
Horizontal angle LPA (degrees)	=	34	-	77	$e^{-age/1}$
Vertical angle RPA (degrees)	=	-9	+	10	$e^{-age/12}$
Vertical angle LPA (degrees)	=	23	+	27	$e^{-age/3}$
Radius of curvature for MPA (mm)	=	43	-	31	$e^{-age/24}$
Radius of curvature for RPA (mm)	=	88	-	49	$e^{-age/18}$
Radius of curvature for LPA (mm)	=	41	+	69	$e^{-age/15}$

Fig14. Age vs. radius of curvature (RC).

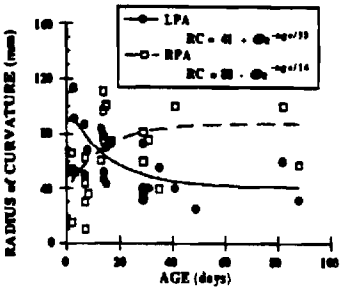

Fig 15: Age vs. area branching ratios.

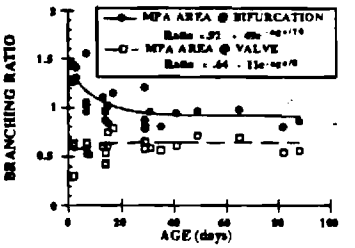

FINITE ELEMENT ANALYSIS (FEM): The natural progression of the *in vivo, in situ, in vitro* approach used in this project is the addition of a computational fluid dynamics component. Preparation began when Rudy Zalesak, a Biomedical Engineering graduate student associated with this research, attended a supercomputer workshop at the University of Pittsburgh that provided an introduction to Dr. Charles Peskin's modeling approach [79] and to a finite element package designed for studying flow problems (Fluid Dynamics Analysis Package). This experience was followed by a three-day FIDAP workshop offered by Fluid Dynamics International. We also received two small grants from the Cray corporation ($7000 each plus computer time on the Cray Y-MP located at the North Carolina Supercomputer Center) to begin these studies. A technique has been developed to transfer necessary structural information obtained from the CT scanned casts to the supercomputer via the 3D computer reconstruction technique developed as part of this project and described above in some detail. Mesh key points can be selected from the original volume rendered images or from the mathematically reconstructed models. The approach to be taken in the FEM studies, which were not part of the original proposal, is described in detail in the Methods Section. The ability to quickly render geometry into a defining mesh and transport that data between computers does, however, represent significant progress toward the goals of the proposed studies--which focus on the importance of the geometry of the surgical options.

THREE CHANNEL SPECTRUM ANALYZER: One of the frustrations of monitoring *in vivo* studies is the need to see 3 channels of spectrum analyzer data--for the main, right and left PAs. We now have a switching box to direct appropriate signal pairs to the Angioscan III system currently in use--which takes time and is

somewhat limited by a 40KHz frequency range. Therefore, we submitted a request for a minority supplement to support work on a three channel spectrum analyzer, i.e., a system that could sample the three sets of quadrature data at the pulse repetition frequency of the 20MHz Doppler system (62.5 KHz),[80] take Fourier transforms, and display the results in real time--an ideal project for a biomedical engineering student (Hiawatha Demby) with a strong background in PC technology. We originally planned to modify an existing PC, but decided to configure an entirely new system given the current low cost of new technology. The system is composed of an IBM 486 33MHz PC clone with an 80 MB SCSI hard disk, 8MB RAM memory, 3.5" and 5.25" floppy drives, a high resolution VGA monitor and display card, and a 12 bit A/D with potential for 1MHz throughput. The system, assembled from parts to assure the optimum configuration and economy, is operational, and software has been written to sample and display data, though optimum A/D rates have not yet been achieved. The first step is to build 3 channel (6 signals) spectrum analyzer. Once that goal is achieved, attempts will be made to process the spectra obtained to create analog type velocity signals based on first moment averaging techniques.[81-82]

SUMMARY: Progress made in the initial period of this project has paved the way for the studies proposed, with respect to techniques developed and to information obtained relative to the maturation of the pulmonary bifurcation of normal lambs. The *in vivo* work has established the normal maturation of physiologic changes--heart rate, pressures, velocities, etc.; the *in situ* work has provided a clear picture of the geometric changes; and the *in vitro* work has allowed us to examine more closely the relationships between geometry and fluid dynamics, both qualitatiavely and quantitatively.

IV. PUBLICATIONS RESULTING TOTALLY OR IN PART FROM THIS RESEARCH

(Animals from these series have often provided control data for publications delineating effects of altered pulmonary hemodynamics.)

a. Carroll SL, Henry GW, Katayama H, Zalesak R, Ferreiro J, Lucas CL, Singh M, Ha B, Lynch PG, Yoganathan AP. Flow visualization in anatomically accurate, flow-through models of the main pulmonary artery trunk. In: Physiol. Fluid Dynamics III, Swamy NVC, Singh M, eds. Narosa Publishing House, 1992, pp 44-49.

b. Ha B, Lucas C, Henry GW, Frantz E, Zalesak R, Ferreiro J, Wilcox B. Pulmonary input impedance estimation using the ARMA model. FASEB J 4:A1076, 1990.

c. Ha B, Lucas CL, Henry GW, Ferreiro JI, Zalesak R, Wilcox BR. Techniques for assessing pulmonary input impedance. In Schneck D, Lucas C (eds), New Frontiers. New York University Press, 1990, pp 281-288.

d. Ha B, Lucas CL, Henry GW, Frantz EG, Ferreiro JI, Severi R, Wilcox BR. Comparison of techniques for assessing pulmonary input impedance spectra. Proc 11th Annual Conf IEEE/EMBS 11:108-109, 1989.

e. Ha B. Techniques for assessing pulmonary input impedance spectrum. Ph.D. Dissertation, The University of North Carolina at Chapel Hill, December 1989.

f. Ha B, Lucas CL, Henry GW, Yoganathan AP, Ferreiro JI, Wilcox BR. Two-dimensional pulmonary artery velocity profiles in growing lambs. Proc 12th Annual Conf. IEEE, Inc. 12:519-520, 1990.

g. Henry GW. Perioperative management of the child with pulmonary hypertension and congenital heart disease. In Harned HS Jr (ed), Pulmonary Heart Disease in the Young. Boston: Little, Brown, 1990, pp 355-375.

h. Katayama H, Carroll S, Zalesak R, Ha B, Lucas C, Ferreiro J, Henry W, Singh M. An anatomically accurate flow-through model of the pulmonary vasculature. Med and Biological Engr 29:247, 1991.

i. Katayama H, Henry GW, Lucas CL, Ha B, Ferreiro JI, Frantz EG and Krzeski R. Three-dimensional visualization of pulmonary blood flow velocity profiles in lambs. Med Biol Eng 29:246, 1991.

j. Katayama H, Henry GW, Lucas CL, Ha B, Ferreiro JI, Frantz EG, Krzeski R. Three-dimensional visualization of pulmonary blood flow velocity profiles in lambs. Japanese Heart J 33:95-111, 1992.

k. Long WA, Henry GW, Lucas CL. New directions in the investigation of pulmonary hypertension in children. In Harned HS Jr (ed), Pulmonary Heart Disease in the Young. Boston: Little, Brown, 1990, pp 379-398.

l. Long WA, Henry GW. Autonomic and central neuroregulation of fetal cardiovascular function. In Polin RA, Fox WW (eds), Fetal and Neonatal Physiology. Philadelphia: WB Saunders, 1991, pp 629-645.

m. Lucas CL, Henry GW, Frantz EG, Ha B, Ferreiro JI, Wilcox BR. Ultrasonic assessment of pulmonary artery velocity patterns. Abstr First World Congr Biomech II:278, 1990.

n. Lucas CL, Wilcox BR, Henry GW, Ferreiro JI, Singh M. Influence of posture variation on fluid flow patterns in a curved tube. Biorheology 27:797-805, 1990.

o. Lynch PG, Yoganathan AP, Ha B, Henry GW, Lucas CL. The effects of curvature on fluid flow fields in pulmonary artery models: flow visualization studies. Med Biol Engr 29:691, 1991..

p. Lynch PG, Yoganathan AP, Ha B, Henry GW, Lucas CL. The effects of curvature on fluid flow fields in pulmonary artery models: flow visualization studies. JBiomech Engr (in press).

q. Singh M, Lucas CL, Henry GW, Ferreiro JI, Wilcox BR. Multiangle visualization of flow patterns in saccular aneurysms. Biorheology 28:333-339, 1991.

r. Singh M, Lucas CL, Henry GW, Ferreiro JI, Wilcox BR. Multiangle visualization of flow patterns in arterial bifurcation models. Biorheology 27:969-970, 1990.

s. Singh M, Lucas C, Henry GW, Ferreiro JI, Wilcox BR. Three-dimensional visualization of the influence of an aneurysm on flow through curved vessels. Proc 6th Internat Conf Biomed Eng, Singapore, 1990, pp 541-544.

t. Sung HW, Yoganathan AP. Secondary flow velocity pattern in a pulmonary artery model with varying degrees of valvular pulmonic stenosis: pulsatile *in vitro* studies. J Biomech Eng 12:88-92, 1990.

u. Sung HW, Lynch P, Yoganathan AP. Studies in pulmonary artery models. Abstr First World Congr Biomech II:304, 1990.

v. Sung HW, Yoganathan AP. Axial flow velocity pattern in a pulmonary artery model with varying degrees of valvular pulmonic stenosis: pulsatile *in vitro* studies. J Biomech 23:565-578, 1990.

w. Zhao C, Ha B, Henry GW, Ferreiro JI, Lucas C, Wilcox BR. Computation of three-dimensional geometric features for pulmonary artery bifurcation. FASEB J 5:A1026, 1991.

x. Lucas CL, Ha B, Henry GW, Frantz EG, Katayama H, Ferreiro JI, Wilcox BR. Frequency domain characteristics of the pulmonary circulation of lambs: animal and computer models. Invited for the 3rd Annual Conference of the Biomedical Engineering Society, Salt Lake City, October 1992.

y. Zhao C, Ha B, Katayama H, Krzeski R, Henry G, Ferreiro J, Lucas C, Wilcox B. Evaluation of the maturation of pulmonary artery geometry. FASEB J 6:A2045, 1992.

z. Ha B, Katayama H, Krzeski R, Lucas CL, Henry GW, Lynch P, Yoganathan AP, Ferreiro JI, Wilcox BR. Pulmonary artery velocity profiles in young lambs. Proc of 9th Engineering Mechanics Conf. LD Lutes, JM Niedzwecki (eds). Am Soc of Civil Engineers, New York, 836-839, 1992.

aa. Ha B, Lucas CL, Henry GW, Frantz EG, Ferreiro JI, Wilcox BR. Effects of chronically elevated artery pressure and flow on right ventricular afterload. In revision for J Appl Phys.

bb. Ha B, Lucas CL, Henry GW, Frantz EG, Ferreiro JI, Katayama H, Wilcox BR. Reflection as a cause of shortened acceleration time in pulmonary lambs with pulmonary hypertension. Submitted for presentation at the 3rd Annual Conference of the Biomedical Engineering Society, Salt Lake City, October 1992.

cc. Lucas C, Henry GW, Frantz E, Ha B, Ferreiro J, Wilcox B. Pulmonary input impedance spectra in the branch pulmonary arteries of lambs with altered pulmonary hemodynamics. Submitted for presentation at the meeting of the Cardiovascular System Dynamics Society, Kobe, Japan, September 1992.

dd. Lucas CL, Henry GW, Ha B, Ferreiro JI, Frantz EG, Wilcox BR. Pulmonary blood velocity patterns in lamb models of pulmonary vascular impairment. Submitted to the International Journal of Cardiology.

ee. Carroll SL, Katayama H, Henry GW, Ferreiro J, Zalesak R, Ha B, Lucas CL, Singh M, Ha B, Lynch PG, Yoganathan AP. Flow visualization in anatomically accurate, flow-through models of the main pulmonary artery. Cardiol Young 2:114-120, 1992.

ff. Katayama H, Krzeski R, Frantz EG, Ferreiro JI, Lucas CL, Ha B, Henry GW. Induction of right ventricular hypertrophy with obstructing balloon catheter: Non-surgical ventricular preparation for arterial switch operation with simple transposition. Manuscript and abstract submitted to American Heart Association for consideration for presentation and Young Investigator's Award at the fall 1992 meeting.

gg. Lucas CL, Ha B, Henry GW, Ferreiro JI, Wilcox BR. Determinants of the pulmonary input impedance spectrum: a model study. Manuscript being revised for Annals of Biomedical Engineering.

4. EXPERIMENTAL DESIGN & METHODS.

The studies proposed are designed to provide answers/insights to the basic questions posed above, i.e., Question #1: *how do conduit design and shape effect shear stresses, secondary flow and flow separation?* Question #2: *how do curves, kinks, pouches, bends, etc., effect pressure/energy losses?* and Question #3: *how do anastomotic geometries (size, angle, relative placements and compliances, etc.) influence flow distribution to a parallel system?* Whether *in vivo, in vitro,* or in the computer, data collection protocols have the same format: 1) flow-mapping to measure velocity patterns, flow separation regions, etc., i.e., to deal with Question #1; 2) pressure-mapping to evaluate energy losses at cavities, corners and stenoses, etc., i.e. to deal with Question #2; and 3) blood flow measurements to quantify the flow to right and left lungs, i.e., to deal with Question #3.

Performing complete studies in all pertinent models available for this work and in all interesting permutations of those models is not feasible or practical in the time period proposed. Thus studies will focus on two age groups: 1 month (10-14) kgs and 3 months (20-25 kgs). One month has been chosen as the starting age because geometries will be large enough to perform the *in vivo* surgery needed and the relevant models for *in vitro* studies can be used to scale. Three months represents a doubling in body weight and the end of the rapid growth phase. As for the normal cardiopulmonary geometry studies, we hypothesize that our results will show that geometry, particularly curvature and connection angles, can play a key role in determining the success of interventions taken to establish and/or improve pulmonary blood flow.

AIM 1--*IN VIVO* STUDIES. One and 3 month old lambs will be selected for study. Procedural steps are as follows: 1) anesthetize and instrument the animal, 2) obtain a set of control hemodynamic measurements, 3) perform a "modified Fontan" type surgical intervention, 4) obtain a second set of hemodynamic measurements, 5) perturb the system, e.g., interrupt conduction patterns, and 6) obtain a third set of hemodynamic measurements. Hemodynamic studies will be altered to fit the model, e.g., measurements will not be made in the MPA if it has been ligated. Our goal is to obtain hemodynamic data and complete casts in at least 12 animals (6 "modified Fontan" procedures at the two ages specified).

Surgical Preparation and Instrumentation. Lambs will be sedated with sodium brevital (5mg/kg), intubated with a cuffed endotracheal tube, and ventilated with a volume cycle ventilator at a rate and tidal volume adjusted to maintain optimal arterial blood gas tensions. The lambs will be anesthetized with a mixture of 1.5 to 0.5% halothane in 100% oxygen for induction and maintenance, respectively. Using a mid-sternotomy approach, the pericardium will be incised and the ascending aorta and main, left and right pulmonary arteries exposed. A fluid-filled polypropylene catheter will be inserted into the femoral vein and advanced to the vena cava. Central venous pressure will be measured with a Statham P23Gb transducer. A Millar Mikro-Tip pressure transducer catheter will be introduced in the femoral artery and advanced to the ascending AO. Left atrial pressure will be measured via a polypropylene catheter inserted directly into the chamber and connected to a Statham P23Gb transducer. Pulmonary artery pressure will be measured with a Millar Mikro-Tip pressure transducer catheter threaded into the main or right PA from a side branch of the left PA. Ultrasonic transit-time flow probes (Transonic Systems, Inc.) will be placed on the MPA and AO. Pressures and flows will be measured. Flow probes will be removed for the velocity profile studies.

Additional Pressure and Flow Measurements. The above describes the initial instrumentation procedure followed in current studies in normal lambs where the focus is on velocity patterns in branch arteries with little

attention given to bulk flow rates. For the studies proposed, however, given the importance of distributing blood to both lungs after flow pathways have been surgically altered, we will also measure RPA and LPA flow using the transit-time probes. In cases where the geometry is such that placement of a probe to measure total right PA flow is impossible, estimates will be made based on the difference between MPA and LPA flow. Also, the success of all the interventions considered depends on appropriate pressure/energy sources to drive flow through low pressure circuits. Therefore, in addition to pressures being measured via indwelling lines, a 5 cm long 22-gauge needle connected to a saline-filled stopcock attached to a Millar Mikro-tip pressure transducer will be used to measure pressures via needle punctures at the site of and upstream and downstream from all connection sites.

Dimension Measurements. Using 5-0 prolene sutures or "crazy glue", two pairs of 5 MHz ultrasonic distance crystals which are 2.5 mm in diameter, affixed to a cloth/silastic patch and activated with a 5 MHz pulsed Doppler system (C. J. Hartley, Baylor University), [83] will be positioned 1-2 cm distal from the tip of the anterior pulmonary valve leaflet to measure continuous posterior-anterior and right-left axial dimensions.

Velocity Measurements. The 20 MHz needle probe (a 1 mm^2 piezoelectric crystal with styrofoam backing embedded in epoxy at the tip of an #18-gauge spinal needle) will be introduced into the MPA 2 cm distal to the tip of the anterior pulmonary valve leaflet, with the crystal directed toward the pulmonary valve (ultrasound pulses oriented 0 degrees to the flow). After introduction, the probe, which is marked in 2 mm increments from the crystal, will be advanced manually toward the posterior wall until a rapid drop in velocity is observed in conjunction with manually felt probe resistance. The spectrally analyzed velocity waveforms will be monitored on an Angioscan II system (Unigon) to verify that measurements are not affected by significant noise bands and that frequency aliasing is not occurring. Due to the size of the sample volume (1 mm^3) and the pulsating movement of the vessel, accurate measurement of velocities near walls are not possible using this technique. However, the pattern observed on the spectrum analyzer unmistakably shows when the probe is at the wall: the range of velocities in one sample volume goes from 0 to values as high as those observed midstream. Once the boundary layer is observed, movement of the probe by 2 mm shows a spectrum with a very narrow band during systole. Sequential velocity measurements will be obtained by moving the crystal in 2 mm increments from the posterior wall to the anterior wall and back. The ultrasonic data will be processed with a zero-crosser whose output will be sampled simultaneously with the pressure data and flow data. The axes of the velocity measurements will correspond to the axes from which dimensions are measured.

At each site, signals will be sampled for 10.24 seconds at a rate of 200 samples per second (2048 samples, Data Translation 2782) and stored on floppy diskettes for later processing (PDP 11/73). The two channels of quadrature data will also be recorded on a Hewlett-Packard 3968A Instrumentation Recorder or through the stereo hi-fi audio inputs of the JVC HRD-470U videocassette recorder for later replay and/or processing. Limited on-line analyses (mean, minimum, maximum) will be performed to verify the general quality of the data and the stability of the preparation.

After the profile is examined along this posterior to anterior wall axis (P-A axis), the needle will be removed from the vessel and repositioned 90 degrees to the left to measure the profile along a right to left wall axis (R-L axis). As was done in the study of the P-A axis, sequential velocity measurements will be made by moving the crystal in 2 mm increments from the right wall to the left wall.

Phasic blood velocity in the branch pulmonary arteries will be measured with extraluminal, bidirectional, 1 (or 2) mm^2 piezeoelectric crystals mounted at a 45° angle on a cloth/silastic patch and activated with a 20 (or 10) MHz pulsed Doppler velocimeter (C.J. Hartley, Baylor University).[84-85] With each crystal oriented antero-superiorly, patch probes will be mounted on each branch PA just distal to the bifurcation junction. Sequential Doppler shift measurements will be obtained by range-gating the pulsed Doppler signal across each vessel in 1 mm increments from the anterior wall to the posterior wall and back.

Color flow mappings (Quantum Angiodynography) will be made of pulmonary and conduit velocity patterns. [24,86] These mappings will be used 1) to verify (qualitatively) the velocity patterns measured with the needle and patch probes and 2) to begin studying flow patterns within extracardiac conduits.

Surgical Interventions. Interventions to be attempted include modified Fontan procedures that we have either investigated or deem feasible without cardiopulmonary bypass in a terminal study in normal, healthy lambs.

Conduits between right and left atria (ASD model) and between right and left ventricles (VSD model) have already been successfully implanted in a series of dogs [87] and lambs [unpublished]. Return via the sizeable azygos vein found in lambs facilitates efforts that require clamping the IVC. If bypass should be necessary to obtain intraoperative survival, the equipment (Sarns rotary bypass pump) and expertise are available in our laboratory. Anastomoses between carotid arteries and jugular veins have been performed successfully in approximately 20 newborn lambs. Brief descriptions of planned procedures are:

Atriopulmonary Connection. The distal end of an appropriate sized Dacron tube graft will be sewn end-to-side to the distal main pulmonary artery using a partial occluding vascular clamp and continuous 6-O prolene suture. The proximal end will be inserted into the mid right atrial wall after excising an ellipse of atrial wall from the leftward aspect of the appendage.(Fig 16A) Air will be evacuated from the conduit and all right heart flow will be diverted through the conduit by occlusion of the proximal pulmonary artery with surgical tape.[88]

Cavopulmonary Connections. Several configurations of cavopulmonary connections will be examined. All begin with an end-to-side or end-to-end anastomosis from the cephalad end of the SVC to the right PA. All flow will be diverted to the left lung during this manipulation and a bypass conduit between the SVC and the right atrium will be used. Configurations for IVC flow include: SVC-RPA-SVC, (Fig 16C) SVC-RPA and IVC-LPA/MPA. (Fig 16D) [21] For total right heart bypass, the IVC will be ligated, extended via a conduit and attached to the inferior aspect of the right PA, left PA or at the bifurcation. (Fig 16E) [89]

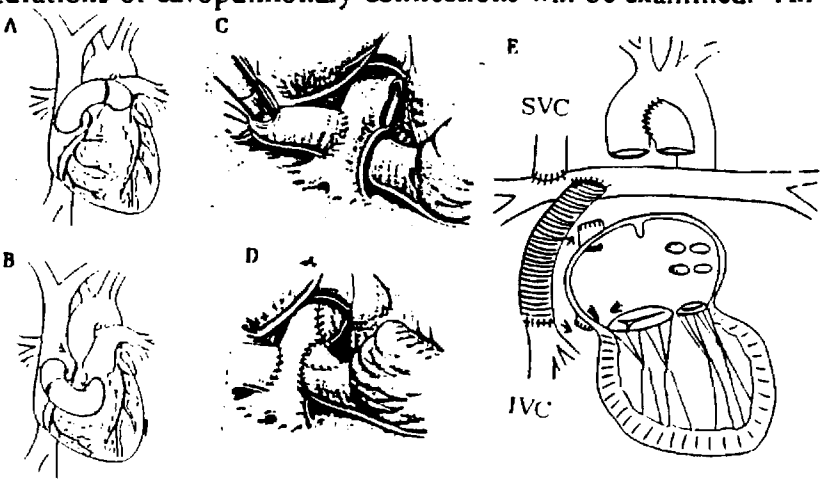

Fig 16. Various types of surgical connections. A=atriopulmonary connections. B=atrioventricular connection [88] C, D=cavopulmonary connections (SVC-RPA-SVC) [21] E=total right heart bypass (SVC-RPA, IVC-MPA) [89]

Perturbations. To test the importance of upstream pressures, abnormal atrioventricular conduction patterns will be obtained via temporary transvenous atrial and ventricular pacing electrodes inserted in the usual manner. Atrial fibrillation will be obtained by overdriving the atrial electrode. The AV node will be ablated and different patterns of AV dissociation will be tested. Pulmonary veins will be occluded to test the influence of downstream pressure.

Technical Considerations. Whenever possible, we prefer to measure velocity with the 20 MHz pulsed Doppler system (high energy, high signal-to-noise ratio). However, the range of these crystals is only 12 mm; therefore, 10 MHz crystals (range = 20 mm) will be used to measure velocity in the branch arteries of the larger animals. The monitoring and data collection procedures for Doppler data are given in terms of our current protocol. However, we plan to have a system developed by the time these studies are initiated that will enable us to view three spectral signals simultaneously, store the spectral data, and output analog "first moment average" signals comparable to the zero-crosser signal. We have also designed and had built a right angle needle probe which will facilitate measuring profiles along the R-L axis in larger animals. We will continue to try to improve and miniaturize the instrumentation.

Data Processing

Velocity Profiles. The velocity of blood at each position [v(x,t)] will be estimated from the waveforms obtained from the zero-crosser using the Doppler equation:

$$v(x,t) = [\Delta f(x,t) \cdot C] \; / \; [2F_0 \cdot \cos(\phi)]$$

where Δf = frequency of Doppler shift, C = velocity of sound in blood = 1.55×10^5 cm/sec, F_0 = frequency of Doppler used = 10×10^6 or 20×10^6 Hz, ϕ = angle of intersection between the Doppler beam and the axis of the vessel = 0° for needle probe or = 45° for extraluminal probe.

A signal averaging technique based on Fourier analyses of each beat in an integral number of respiratory cycles [90] will be used to obtain a representative waveform for each sampling site. These waveforms can then be used to project a profile along an axis (e.g., Fig 10) and, assuming linear variations in velocity with arc length along a concentric ellipse model of the MPA (Fig 17), can be combined to project 3D instantaneous profiles and estimates of blood flow. [91] (Appendix 6)

Input Impedance. For purposes of calculating input impedance, the auto spectral density of the velocity or flow waveform and the cross-spectral density between PA pressure and velocity or flow waveforms are also computed on a harmonic basis for each of the M beats and the results averaged. Input impedance at each harmonic is calculated as: the cross spectral density/auto spectral density.[90] The complex results will be displayed in modulus and phase form. The spectra will be evaluated for changes in shape, e.g., shifts in the frequency of the first modulus minimum, as was done by Greenwald, Johnson and Haworth [92] for the newborn and infant pig. Data obtained from the measured PA flows will be analyzed in more detail and parameters such as characteristic impedance, pulse wave velocity and indices of pulse wave reflection calculated. Investigators [93-95] have documented that application of a tight, circular, rigid electromagnetic flow probe around the compliant PA affects the pressure tracing and velocity patterns. Use of the new transit-time probes minimizes vessel distortion because the vessel needs to fill only 50% of the internal cross-sectional area of the probe for the probe to function properly. These probes provide a more accurate assessment of bulk flow: 1) probes have a stable zero and are thus not subject to baseline drift and 2) accuracy does not depend on the assumption of a symmetric velocity profile.[96]. We will continue to calculate impedance whenever feasible, recognizing such computations will not be possible in steady flow studies.

Compliance. MPA compliance will be estimated from the slope(s) of pressure-volume curves generated by assuming that the two measured axial dimensions are the major and minor axes of an ellipse. These values will be used to describe any changes in the pulmonary arteries as a result of surgical interventions.

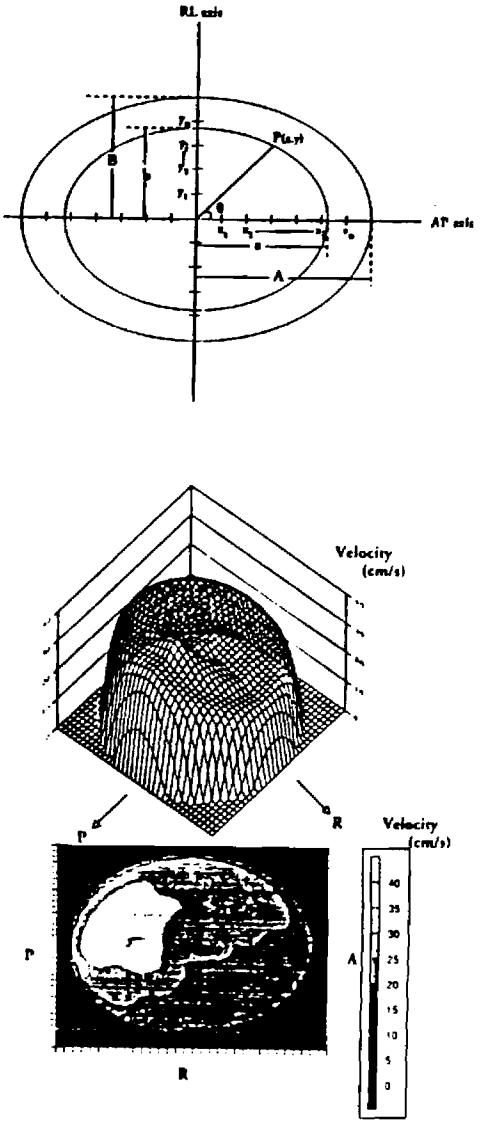

Fig 17. Technique used to determine 3D pulmonary artery velocity profile. Elliptical model used to determine velocity at a point P(X,Y) not measured directly with ultrasound probe. 3D image of pulmonary velocity profile represented by wireframe and contour imaging.

AIM 2--*IN SITU* STUDIES. The external circumference of the MPA will be measured 1 cm above the pulmonic valve. Surgical tapes will be placed around the superior vena cavae (SVC) and the inferior vena cavae (IVC). The SVC (and IVC if SVC and IVC pathways do not merge at the atrial level) will be cannulated with a large-bore polypropylene catheter. Prior to exsanguination, the lambs will be given sodium heparin (200 units/kg). The lambs will be exsanguinated through the femoral artery and the blood volume will be simultaneously replaced with heparinized saline through the femoral vein. When the hematocrit reaches 4%, a massive dose of sodium pentobarbital will be administered in order to cause death. The SVC and IVC will be ligated. Nitrogen will be introduced under pressure through the right atrial appendage to dry the pulmonary vasculature.

A highly viscous solution of silicone rubber compound will be injected through the large-bore catheter in the SVC (and IVC if necessary) at physiologic pressures to obtain a cast of the caval connections, conduits, right heart, and pulmonary artery bifurcation. Prior to harvesting, the cast will be allowed to cure. After curing, the casted structures will be placed in 2N KOH to remove the lung and heart tissue from around the cast. The silicone rubber cast will be placed in a casting box (Teflon), and an optically clear plastic (e.g., Bio-Plastic,Wards Natural Science, Rochester, NY) will be poured around the rubber cast. When polymerization is

complete, the mold will be removed from the casting box and the flexible cast will be pulled from the plastic mold. To determine 1) if the injection pressures were realistic and 2) the amount of resin shrinkage, the external circumference of the MPA will again be measured 1 cm above the pulmonic valve and the result compared with the measurement obtained *in vivo*. Conduit and connection areas will be cut and respliced to retain shape during the curing process but to "give" when the cast is removed after the mold is cured. The machine shop will drill holes to open flow channels, add attachments for mounting external tubing and taps for pressure and/or velocity measurements, and close the tricuspid valve area in models of pulmonary atresia.

Homografts for *in vitro* studies will be harvested from lambs first used for other purposes. The MPA, portions of the branch PAs, the ascending aorta, and the related valves will be removed and preserved in an antibiotic solution kept at 4°C. Given an ongoing collaboration with Cryolife Inc., Marietta, Georgia, we will attempt to have some homografts cryopreserved.

AIM 3--*IN VITRO* STUDIES: Although conducting the velocity measurements *in vivo* is most realistic, the complexity of such a model can affect the outcome. For example, it is not possible to alter geometry and hemodynamic parameters, such as heart rate, cardiac output and PA pressure, over a sufficiently realistic anatomic and physiologic range in the *in vivo* animal models. We therefore plan to test the hypothesis that the interaction between cardiopulmonary and conduit geometry plays an important role in determining the success of Fontan type operations using *in vitro* models of the right heart that will allow 1) deliberate variation of conduit geometry while cardiopulmonary geometry and physiologic parameters are kept constant; 2) deliberate variation of cardiopulmonary geometry while conduit geometry and physiologic parameters are kept constant, and 3) deliberate variation of physiologic parameters, such as heart rate, systolic duration, cardiac output and PA pressure, while geometries are kept constant. Furthermore, *in vitro* studies allow measurement of velocity patterns near the walls of the vessels (resolution=0.3 mm^3), which is not possible *in vivo* using currently available technology (resolution = 1 mm^3). Lack of this capability has led most investigators of the fluid dynamic mechanisms of atherosclerosis to focus their attentions on *in vitro* studies.

Models to be studied come under three general categories: 1) anatomically exact flow-through models, 2) modifications of existing models to include subvalvular tunnels and alterations in vessel geometries comparable to those observed in patients with sub- and/or supra-valvular pulmonic stenosis, and 3) mock-ups of right heart-pulmonary artery connections made from a) conduits of commercially available materials and homografts and b) geometries provided by available casts of right heart and pulmonary arteries of lambs ranging in age from 1 day to 6 months. Flow mapping techniques likewise fall into three general categories: 1) flow visualization (FV) including dye injection and laser light scattering, 2) pulsed Doppler ultrasound (PDU), including color flow mapping, and 3) laser Doppler anemometry (LDA).

In vitro pressure mapping studies will be conducted via wall taps located at various model locations in the "connection models". If necessary the pressure mapping studies will be conducted using Millar pressure transducer catheters. During these studies volumetric flow rates in the main and branch connections will be measured using Carolina Medical electromagnetic flow probes.

Models:

Anatomically Exact Models: Cardiopulmonary and connection geometries provided by the silicone rubber molds (described in the *in situ* studies) will be used in clear resin models that will facilate flow visualization as well as LDA velocity measurements. Physiologic parameters will be varied, but the primary focus will be on obtaining additional flow mapping (PDU & LDA) information for conditions matching the *in vivo* situation.

Sub- and Supra-Valvular Pulmonic Stenosis Models: These studies are an extension of work previously performed by Dr. Yoganathan et. al. using the flat model of the adult human pulmonary artery and outflow tract.[53] (Appendix 7) Custom-made subvalvular tunnels of varying lengths and cross sections were placed in the outflow tract and pressure-mapping and velocity studies were performed, relating pressure gradients to gradients predicted by measuring velocities. We propose to extend this work by modifing existing models of the 1 and 3 month old lambs in the same fashion. Supra-valvular stenosis will be examined by selectively narrowing the main or a branch PA, using designs illustrated by Franch and Gay (Fig 18) [97] and studying the alterations in velocity patterns and pressures. Studies, to be conducted with a Vingmed SD 100 system using 2.0, 3.5 and 10 MHz transducers, will also focus on the degrees/levels of turbulence. High levels of turbulence

can and will lead to MPA, LPA and RPA dilation and changes in the bifurcation geometry (such as the tent pole effect). The pressure-mapping studies will reveal the location of maximal pressure drop (i.e., which lesion/defect is dominant) This is critical, since due to pressure recovery effects, the pressure drops across a series of stenoses are not necessarily additive.

Mock-Up Models: By the end of the initial phase, we will have identified a series of casts, one from each of the age groups studied, that is representative of normal growth and development of the right heart and pulmonary arteries of lambs. Glass models of the outflow tract, MPA, and branch PAs will also be available. We will begin with studies in 1 month and 3 month old models. Other ages will be considered if this approach proves enlightening. Glass representations will be made of the right atrium and ventricle that can be appropriately positioned and connected to the outflow/arterial sections. The connection between the chambers will be made to open or close, depending on the study. An abridged glass artery model consisting of the bifurcation area and branch arteries will be made for ventropulmonary studies. A surgeon will select the conduit diameter and length felt most appropriate for making atriopulmonary and atrioventricular connections in each model. The best size for ventropulmonary connections is assumed to be the size of the existing MPA.

For each age, five models will be fabricated with openings formed for the following connections: 1) small atriopulmonary connection, 2) small atrioventricular connection, 3) large atriopulmonary connection, 4) large atrioventricular connection and 5) ventropulmonary connection. (Efforts will be made to accomplish this using one multipurpose model with a standard opening that can be closed or altered in size via appropriate conduit fittings.) Studies will be performed using corrugated Dacron, PTFE and homografts. The geometry of selected conduits in their *in situ* position will also be approximated with glass for flow visualization. To improve refractory properties for flow visualization, the model may be placed in a water-filled plexiglass box. Cause and effect relationships will be studied by the following mechanisms: 1) conduit size by placing small conduits in large geometries and vice versa, 2) curves and bends by increasing and decreasing the lengths of the conduits, 3) wall perturbations by examining corrugated vs smooth wall designs, 4) compliance by using homografts compared to synthetic materials, 5) branching angles by varying the angle at which the conduits are attached to the bifurcation model, 6) pouches by bypassing the right atrial chamber, etc.

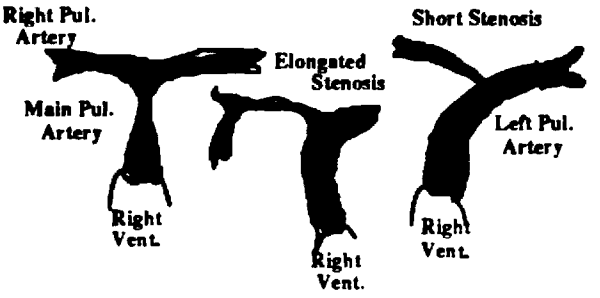

Fig 18. Examples of supra-stenotic patterns to be tested.

Procedures

All models, with the exception of conduits made of actual materials that can be studied only via Doppler ultrasound techniques, will be appropriate for flow visualization studies. LDA velocity measurements will be conducted in selected models in order to obtain more detailed and spatially accurate velocity information not obtainable by Doppler ultrasound techniques.

All of the *in vitro* flow studies requiring pulsatile flow will be conducted on the Georgia Tech right heart pulse duplicator system. Components include: three electromagnetic flow probe (Carolina Medical Electronics EP 680) and pressure taps, three flow control valves, pulmonic pressure wave control (PPWC) section on both the right and left branches of the PA model, a PPWC air reservoir, an atrial reservoir, a straight valve section, a right ventricular bulb, a ventricular pressure wave control (VPWC) section, a VPWC air reservoir, an immersible centrifugal pump (Little Giant), and a plastic bucket. The latter two items are used for emptying and filling the pulse duplicator. A blood analog fluid (45% by weight aqueous glycerine solution, density= 1.10 g/cm^3,viscosity= 0.035 poise) will be used as the working fluid.

The system is versatile and can mimic a wide range of physiologic conditions--for example: heart rate from 30 to 150 beats/min; cardiac output from 1.0 to 10.0 liters/min; mean PA pressure from 15 to 150 mm Hg. The models will be placed in the right heart pulse duplicator system. With each model, experiments will be conducted at three heart rates, three cardiac outputs, and three mean PA pressures, consistent with the physiologic ranges of the animals in the related age group.

Porcine trileaflet (aortic or pulmonic) valves (stored in antibiotic solution) of variable sizes that can be used to simulate normal pulmonary valves are available for these studies. The valves will be mounted in a transparent silicone rubber tube with sinuses (both appropriately sized) in a manner similar to the way a cardiac surgeon would sew a homograft (aortic or pulmonic) in a human pulmonary artery. We have developed the above technique as part of an on-going research project in collaboration with the FDA and Medtronic to evaluate the fluid mechanics of nonstented aortic valve heterografts.

Given the nonpulsatile nature of flow in cavo- and atriopulmonary connections, many of the models will be studied under conditions of steady flow, for which dye studies are particularly appropriate.

Flow Visualization (FV) Studies. Studies will be conducted using 7 mW He-Ne lasers and white-light as the light source. The laser beam is converted into a plane of light by directing it through a glass rod. Adjustments will be made so that the sheet of light (1 to 2 mm in width) can pass through the desired cross-section for flow visualization. Tracer particles consisting of Amberlite particles (100 microns in diameter) or glass beads (10 microns in diameter), will be added to the blood analog fluid to act as light scatterers. Flow visualization (FV) studies with fluorescent tracer dyes such as sodium fluorescein will also be conducted. A Canon A-1 camera with a macro lens, electro-pneumatically triggered by the pulsed duplicator electronics, will be used to obtain photographs of the flow patterns in the models. Studies in two orthogonal planes, i.e., in the plane of the bifurcation and in a perpendicular plane, will be conducted with all the models as appropriate. The FV studies will be recorded on video tape using a Panasonic video camera (model 5100) and on 35 mm film using a Canon A-1 camera (with a macro lens) electronically triggered by the pulse duplicator electronics.

The FV studies will be used to evaluate the flow field globally, and more specifically to identify regions of flow separation, flow stagnation and disturbed flow. Particle residence time measurements using particle tracking software on Mass Comp Computer system (in Dr. Gidden's laboratory at GIT) will accentuate regions of flow stasis in the connection models, regions considered to have potential to occlude due to thrombus formation and/or fibrotic peel formation.

Pulsed Doppler Ultrasound (PDU) Studies. PDU velocity profile measurements will be made with 10 (and if needed 5) MHz needle probes in two orthogonal planes when appropriate (i.e., L-R and A-P planes). The probes will be interfaced to a VingMed SD-100 ultrasound Doppler system. At each site, the sample volume ($1 mm^3$ in size) of the intraluminal probe (<2mm in diameter) will be range gated to areas of interest and the ultrasound crystal oriented such that the ultrasound beam is parallel to the main direction of flow. For each measurement, 10 to 30 seconds of quadrature ultrasound Doppler data will be recorded on tape for further processing (either on-line or off-line). The Doppler spectral data will be obtained via a fast Fourier transform algorithm on the SD-100 system. The PDU results will also be animated using the Silicon Graphics IRIS 4D/380 computer. "Quantitative" color Doppler flow mapping will be done with a Toshiba 270A or an Acuson system with 5.0 and/or 7.5 MHz transducers. We have developed an image grabbing system using a MAC FX and a Silicon Graphics W-4D25 work station for analyzing the color Doppler images.

Laser Doppler Anemometry (LDA) Studies. The LDA studies will be conducted with a new three dimensional DANTEC fiber-optic system interfaced to a flow analyzer. The LDA system uses a 2W Argon-ion laser and Bragg cells for directional sensitivity. The flow analyzer is interfaced to an Everex 386 micro-processor for on-line data collection. The collected data will be analyzed and animated using a Silicon Graphics IRIS 4D/380 VGX Power Center Graphics Super computer (also recently purchased). The fiber-optic system is capable of creating a sample volume of 0.3 mm in length. The LDA system will be used for 3D velocity mapping in selected models, under steady and pulsatile flow conditions as physiologically appropriate. Two dimensional velocity data (axial and radial) are collected over the entire cardiac cycle. The raw data are stored on magnetic cartridge tape for comparison with the *in vitro* and *in vivo* pulsed Doppler ultrasound measurements. The optical portion of the LDA system is mounted on a traversing mechanism that can be moved in three independent directions to within an accuracy of 0.001 inches. Since the refractive indices of the blood analog fluid and the model will be matched, optical difficulties will be minimized. Also, where necessary, turbulence measurements will be made. The current LDA system (He-Ne DISA 55X) has been shown to be valuable in characterizing velocity and turbulence fields distal to prosthetic heart valves and in *in vitro* work on pulmonic stenosis.[52,52,55] (Appendix 8) To understand the problem of right sided graft failure, wall shear stress measurements (in axial and circumferential directions) will be taken in some models.

AIM 4--*COMPUTATIONAL* STUDIES: Computational studies include the characterization of geometry component developed in the initial phase and a finite element (FEM)/computational fluid mechanics component to be fully developed in the proposed phase. Configurations to be studied will be CT scanned using a GE 9800 scanner. Scanning parameters will include two-second scans at one 140 mA, 120 kV, using a standard reconstruction algorithm and a 512 matrix. These scans will consist of contiguous 1.5 millimeter cuts through the entire cardiac chamber cast. The features to be extracted from the 3D computerized reconstructions of these images--curvature, branching angles, diameters, lengths, tapers, flow divider offsets, etc.--have been described in the Progress Report. Where applicable, the criteria will be the same as those used by Friedman et al. for describing aortic bifurcations.[50] For example, the centerline of the main trunk and branch vessels will be determined. The distance between the bifurcation of the centerlines of the branch arteries and the centerline of the main trunk will be defined as the flow divider offset. Bifurcation angles will be estimated for branch vessels and conduits relative to the intersections of the centerlines. This analysis will be applied to conduits and as many generations of arteries as feasible.

Meshes generated as part of geometry analyses will be transported to the Cray Y-MP at the North Carolina Supercomputer Center (NCSC) and used to define the structure for the FEM studies, to be performed initially using the commercial finite-element flow package, FIDAP. Flow simulations begin by assuming that blood is modeled adequately in large vessels by two equations: the normalized Navier-Stokes equations for Newtonian flows,

$$\frac{\partial u}{\partial t} + u \cdot \text{grad}\, u - \nu \Delta u + \text{grad}\, p = f,$$

where u is the fluid velocity, grad p the pressure gradient force, f the body forces, which can be assumed to be zero in physiological situations, and ν is the kinematic viscosity; and the incompressibility constraint , div u = 0, which is satisfied because blood is an incompressible fluid.

The no-slip condition for a viscous fluid leads to the uniform boundary condition u = 0 along the wall. We also make the assumption that the viscosity is constant and Newtonian. For flows in large vessels, small departures from Newtonian behavior have negligible effects [98].

A physically realistic model of the vessel would also include the compliance due to shape changes and elasticity, as well as the effects of wall tethering. There are great technical obstacles to fully including these effects, although approaches we are taking are discussed below. In the steady-state case, which is most pertinent to our shunt studies, these effects are less important.

The finite-element method we use for simulating physiological flows has the advantage that elements used can be different sizes and shapes, including elements with curved sides. Free-form shapes like blood vessels can be modeled well. Also computational resources can be concentrated on regions needing finer resolution of detail, like the fluid volume near a bifurcation.

The FIDAP computational fluid dynamics package has a mesh generator that allows us to create a finite-element mesh from the geometric mesh derived from our data. The methodology for specifying the boundary conditions and physical constants and obtaining the flow solution using FIDAP differs depending on whether a transient (time-dependent) or steady-state solution is required. Transient flows are the most general case, but require a great deal more computation. Steady-state flows are a good and physiologically realistic model for flow in shunt situations, as in venous-pulmonary shunts, where the flow character tends to be nonpulsatile.

The Steady State Case: In this case the boundary conditions at the inlet, just distal to the valve, are specified by giving the velocity profile across the artery. In modeling steady flow in a normal pulmonary circulation, this profile should be roughly flat, as determined by experimental studies. In the case of venous flow into a shunt, a parabolic profile, characteristic of fully-developed flow, is more accurate.

In either case, the velocities at the branch outlets are not known *a priori* and cannot be used as boundary conditions there. Although outlet boundary conditions are a matter of some controversy [99], a reasonable and common downstream boundary condition is constant pressure. These pressures could be the same at the end of each branch, although specifying different downstream pressures in each branch would model different pulmonary resistances in the right and left pulmonary vasculature.

Once the elements and boundary conditions are specified, the FIDAP solver assembles the algebraic matrix

whose solution determines the approximate flow. Either iteration or a type of direct Gaussian elimination is used by FIDAP to solve the resulting non-symmetric matrix. The latter "segregated" direct method is faster in large 3D problems like the models we consider.

The Pulsatile Case: The method for solving these flows differs from the above in the boundary conditions and in that a method must be chosen to advance each time step. For stability, the method routinely used is a backward implicit scheme. Constant pressure boundary conditions downstream can be used, as in the steady state case, but consideration of the effects of both compliance and reflected waves, as represented by a complex downstream impedance, is more realistic. Such conditions cannot be directly specified in FIDAP, but a simple "modified Windkessel" (RRC circuit) impedance can be simulated by stopping the simulation at each time step, updating the downstream pressure as a function of previous pressure and flow history, then restarting.

Time-dependent flows also bring into focus the lack of elasticity in the numerical model, as discussed above. Some of the effects of elasticity can be simulated by including the Windkessel boundary effects, but it would be preferable to simulate directly the change of shape of the vessel. There are two possible approaches to this problem. The most realistic, but the most difficult, is directly coupling the fluid flow to the elastic properties of the vessel, so that fluid forces act directly to distend the vessel. This approach has been taken for modeling of heart ventricles by Peskin [ref] using his "immersed boundary method". This method involves a complex model of the boundary as a bundle of elastic fibers immersed in a fluid.

A second approach, developed by Reuderink [100] in his thesis modeling fluid flow in the carotid artery bifurcation, uncouples wall motion from local fluid flow. Wall motion is calculated from assumptions about wave propagation and reflection, and then is used to create a moving boundary for the flow solution, updating the boundary position between time steps. This approach resembles the "Windkessel" approach described above. Unfortunately, the FIDAP package is not yet able to handle moving solid boundaries in three dimensions, although it can do so for 2D problems, and 3D capabilities are projected to be available by the next calendar year. We are also investigating the use of other fluid dynamics solvers (such as NEKTON) that have that capability already. It should be noted that Reuderink found that including elasticity in his model caused little qualitative change in the flows fields he calculated, while only decreasing the magnitude of calculated flow extrema and shear rates, consistent with the findings in compliance related studies discussed above.[67-71].

Once the solution is found, both pressure and velocity data are available at each element. FIDAP's postpreocessing tools allow us to extract important information from the solution: first, color rendering of velocities allows identification of regions of flow separation and stagnation, and allows direct comparison with patterns visualized by color doppler flow mapping. Of special physiological interest is the calculation of shear rate near the wall. Shear rate is defined as the rate of change of velocity in a particular direction, and near the wall is defined as the normal derivative of axial (tangential) velocity, i.e, $\tau = \partial v/\partial n$. Streamline visualizaton will allow us to classifly typical flow topologies using "critical point" techniques, an important new tool used in aerospace studies[101-104] but never before to our knowledge used in physiology. Second, pressure mappings can be obtained directly from the data to allow measurement of pressure drop and energy losses. Finally, FIDAP can directly compute flow rates across any boundary of the model, so that model flow distribution can be obtained.

An example of a vector velocity plot in a 2D pulmonary artery bifurcation model under conditions of steady flow is shown in Fig 19. NCSC is developing a tool to allow FIDAP output files to be processed by the AVS visualization system, which will enable simpler coupling between FIDAP and the AVS tools we use to create structural data.

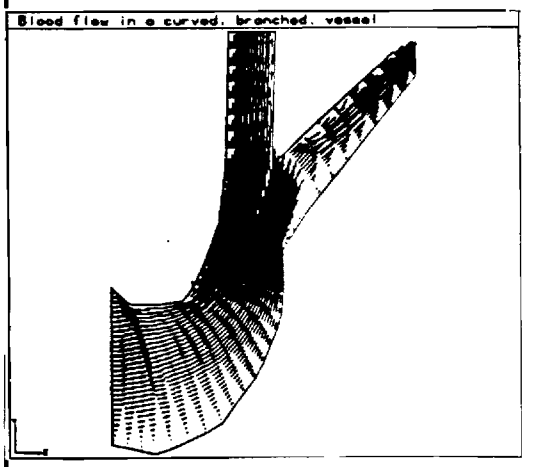

Fig 19. FIDAP vector velocity plot.

AIM 5--CONSOLIDATION: The clinical problem addressed by this proposal is the need for improved methodology for repairing congenital lesions that impede blood flow to the pulmonary circulation. Repair options include creation of cavopulmonary connections and/or implantation of extracardiac conduits. Questions to be considered in implementing these options are: *1) how to prevent conduit failure? 2) how to maintain sufficient energy to move blood through a low pressure system? 3) how to appropriately distribute flow to both lungs? and 4) how to prepare for*

reasonable growth? Answers to these general questions require answers to basic questions: *1) how do conduit design and shape effect flow fields (shear stresses, secondary flow and flow separation, etc.)? 2) how do curves, kinks, pouches, bends, etc., effect pressure/energy losses? and 3) how do anastomotic geometries (size, angle, relative placements, etc.) influence flow distribution to a parallel system?*

The studies proposed are designed to answer these basic questions and provide insights regarding the clinical problems. The combined approach--*in vivo* studies in realistic animal models, *in situ* casting of relevant structures, *in vitro* studies via a variety of techniques, and *computational* studies--will provide a comprehensive picture of the fluid mechanics of many of the current surgical interventions. The studies are united by common geometrical structures and data collection objectives--(i) pressure-mappings, (ii) flow-mappings/velocity patterns, and (iii) flow distribution to right and left lungs. Each technique uniquely contributes to the understanding of the problem at hand as well as to the success of other studies. As for the current phase, a video tape will be prepared to compare results from all studies--animated velocity profiles for *in vivo* work, flow visualization footage for *in vitro* work, 3D displays of CT scans of casts obtained *in situ*, and animations of *computational* fluid dynamic studies.

Data Manipulation and Integration:

In vivo studies provide (i) surgical preparations for *in situ* studies, (ii) hemodynamic measurements for boundary conditions in *computational* studies (upstream velocity profiles, downstream loads, and pressure-diameter relationships), and (iii) hemodynamic measurements for validating findings in *in vitro* and *computational* studies.

In situ studies provide the geometric detail needed for *in vitro* and *computational* studies.

In vitro studies are three pronged: (i) flow visualization (FV), (ii) pulsed Doppler ultrasound (PDU), and (iii) laser Doppler anemometer (LDA)

FV studies will be used to guide quantitative *in vitro* studies, namely the pressure mapping and PDU and LDA velocity studies. The FV results will also help in optimizing the locations for the PDU velocity mapping studies and in selecting the most important models for the LDA velocity studies.

PDU velocity mapping studies will provide the quantitative velocity field information that can be directly compared with the *in vivo* animal studies. Furthermore, *in vitro* pulsed Doppler measurements can be performed over a wide range of anatomic and physiologic conditions not possible *in vivo*.

LDA velocity measurements (3D) will be conducted in selected models and at selected locations based on the FV results and the PDU velocity measurements. These LDA measurements will be used to provide boundary conditions and to validate the findings in selected *computational* studies.

Computational studies: The geometry of the systems to be studied will be provided by the CT scanned casts obtained *in situ*. Boundary conditions will be matched to hemodynamic findings obtained *in vivo* and *in vitro*, and results obtained will be validated accordingly.

Data Interpretation:

Basic Questions:

1) *How do conduit design and shape effect flow fields?* FV studies (analogous to color Doppler flow mapping and MR angiography) provide a global overview and valuable insight to the various flow fields. These studies will identify regions of flow separation, flow reattachment, flow stagnation, disturbed flow and turbulence. Particle residence time measurements will also identify regions of stagnation.

   PDU velocity mapping studies will provide us with the quantitative velocity field information that is most applicable to measurements that can be obtained *in vivo*. LDA measurements will provide detailed insight into the three dimensional, quantitative nature of the flow field, unobtainable by any other means *in vitro* or *in vivo*. LDA measurements provide the capabilities of quantitatively documenting the levels of flow disturbance as well as the wall shear stresses both in the axial and circumferential directions, quantities that are hypothesized to be particularly important in the conduits and the anastomotic sites of the "connection models" (mock-ups and anatomically exact). Geometric features to be considered include connection

patterns, lengths, curvatures angles and wall intrusions (i.e., surface roughness and stenotic lesions). Physiologic parameters to be considered include cardiac output and heart rate.

Computational studies allow even finer resolution of flow field features in relevant geometries, e.g., wall shear rates can be calculated with any desired precision. Moreover, computational studies enable screening of new ideas relative to conduit design. For example, conduits with taper may be preferable to straight conduits. Taper would promote axial flow and deter flow disturbances and turbulence. The absence of significant atherosclerosis in pulmonary arteries has been attributed to the degree of taper present..

2) *How do curves, kinks, pouches, bends, etc., effect pressure/energy losses?* In *in vivo* and *in vitro* studies in the "connection models", the pressure mapping measurements will identify locations of maximum energy loss and will thus permit us to evaluate the energy loss efficiency of different connection geometries used in the clinical arena. Using the mechanical energy balance approach together with the pressure mapping results, it should be possible to optimize the energy loss characteristics of the different "connection models".

Pressure mapping studies performed *in vitro* in models of sub- and/or supra-valvular pulmonic stenosis will provide quantitative information regarding the severity of the sub-and supra-valvular stenoses and identify their interaction and the dominant lesion. The measured pressure gradients (peak and mean systolic) will be related to the PDU measurements via the Bernoulli equation (see Appendix 7). In the case of stenoses in series, a variation of the mechanical energy balance equation will be used to account for pressure recovery effects. It should be noted that the pressure drops across a series of stenoses are not necessarily additive.

The atrioventricular conduction studies will enable us to quantify the importance of atrial contractions as a pressure source under normal hemodynamic conditions and when downstream pressure is elevated by pulmonary venous occlusion.

3) *How do anastomotic geometries (size, angle, relative placements, etc.) influence flow distribution to a parallel system?* The *in vivo* studies will provide initial insight as to the degree to which the atrio- and cavo–pulmonary connections influence blood flow distribution to right and left lungs. Variations will be tested extensively in the *computational* studies, in which downstream boundary conditions are pressure determined.

In the atriopulmonary connections, all systemic venous flow returns to the right atrium, which is then connected via a conduit to the MPA. The position and angle of the conduit anastomosis to the MPA is hypothesized to be the major determinant of flow distribution. In the cavopulmonary connections, the major variation is the manner in which flow returning via the IVC reaches the pulmonary circulation. Flow return via the SVC is commonly channeled to the RPA, i.e., the SVC is ligated and the superior end anastomosed to the superior side of the RPA. IVC routes vary from the connection of the inferior end of the SVC to the inferior side of the RPA (directly opposite the superior side connection) to the total bypass of the right atrium via a conduit connecting the IVC directly to a pulmonary artery. The primary determinant of flow distribution in cavopulmonary connections is hypothesized to be the attachment site of the IVC/caudal end, e.g., anastomosis to the MPA or LPA is hypothesized to promote more flow to the left lung than anastomosis to the RPA. Additional determinants are hypothesized to be the presence/magnitude of atrial contractions and the factors found significant in the atriopulmonary connections, i.e., conduit angles and sizes.

Clinical Problems:

1) *How to prevent conduit failure?* A primary causes of late conduit failure are obstruction secondary to fibromuscular ingrowth, valvular degeneration, and pseudointimal peel formation. We hypothesize that wall shear plays an important role in conduit failure via these mechanisms of obstruction. The wall shear stress measurements will identify regions of low wall shear stress within the graft models. Wall shear is a key rheological factor to elicit the local adaptive response of the vascular wall. Regions of low wall shear have been correlated with the development of anatomic neointimal fibrous hyperplasia in left sided conduits. We could therefore correlate our wall shear measurements with clinically observed graft failures in right sided conduits. Regions of low flow velocity and relative stasis are potential regions for the deposition and interaction of activated and/or damaged blood elements, causing thrombus formation, particularly on artificial cardiac connections. Our flow field measurements should identify such potential

pathophysiologic areas. Our extended study of the manner in which geometric parameters and various types of physiologic connection influence pertinent fluid mechanic features will provide new insight into ways to improve the geometry of the connection and/or to select alternative anatomic locations for the connection placement.

A second cause of late conduit failure is the patient outgrowing the conduit. Techniques to accommodate for patient growth are considered below as a separate problem.

Other factors not addressed by our study also have a significant impact on this problem. For example, recent advances in heparin bonding technology should extend survival times for artificial grafts.

2) *How to maintain sufficient energy to move blood through a low pressure system?* This answer is directly related to basic question #2 above. The pressure mapping studies will indicate which connection designs best preserve the hydraulic energy delivery to the pulmonary vascular bed. Furthermore, *in vitro* pressure mappings together with the PDU measurements will establish the efficacy of using non-invasive echo Doppler measurements in the clinical setting to assess the severity of complex pulmonary artery stenoses.

3) *How to appropriately distribute flow to both lungs?* This answer is directly related to basic question #3 above. The optimal design for a normal animal model is that which best matches presurgical flow distribution with minimal loss of pressure energy.

4) *How to prepare for reasonable growth?* As indicated above, patient growth can be a cause of graft failure. Thus, periodic replacement of implanted homografts or extracardiac conduits is part of the repair process in the young. Based on studies by us and others, the most desirable flow patterns will be obtained with straight tubes. However, even if geometry permitted, straight conduits with no allowance for growth are not practical. *In vitro* and *computational* studies will examine criteria for optimizing the design process, e.g.: (i) lengths that will allow for reasonable projected growth but will not impose curves or bends of a magnitude that enable development of regions of flow separation and/or stagnation (i.e., conduit obstruction regions) and significant energy losses (i.e., pressure drops), (ii) diameters that are optimal to promote uniform axial flow and to minimize regions of stagnation and very low wall shear, and are large enough that demands of increased flow with growth will not create pressure gradients with significant energy losses, (iii) anastomosis angles that meet the size requirements of the connecting vessels but minimize kinks, bends, etc., and thus avoid regions of flow separation. The casts available from the initial phase of this study and the computer model of normal pulmonary artery growth in lambs will enable us to extrapolate findings beyond the 1-3 month age range.

Conclusion: The combined *in vivo, in vitro, in situ* and *computational* studies described in this proposal are essential to our fundamental understanding of the fluid mechanic characteristics of surgical options for repairing impeded pulmonary blood flow in the young. Unification of results obtained should help identify causes of graft failure and assist surgeons in selecting interventions that establish optimal pulmonary blood flow patterns and make appropriate allowances for patient growth.

TIME TABLE: As in the current proposal, we plan to perform *in vivo, in situ, in vitro* and *computational* studies in parallel. For each new *in vivo* model, hemodynamic data will be obtained and an *in situ* cast made that will be CT scanned for computational studies and used as the form for obtaining flow-through models for *in vitro* studies. Comparable studies will be preformed in lambs of two distinctively different sizes and ages. A second series of *in vitro* studies will be performed in variations of existing flow-through models and in mock-ups based on available silicone rubber and methyl methacrylate casts.

Year 1. Models: extracardiac conduits between the right atrium and the main pulmonary artery and between the right atrium and the right ventricle. *In vitro* studies in models of sub- and supra-pulmonary stenosis.

Year 2. Models: Simple cavopulmonary connections.

Year 3. Models: Complex cavopulmonary connections including total right-heart bypass.

Year 4. Completions of studies/series as needed. Analysis and synthesis of results.

9. Literature Cited.

1. Bogren HG, Klipstein RH, Mohaiddin RH, Firmin DVn,Undersood SR, Rees, RSO, Longmore DB. Pulmonary artery distensibility and blood flow patterns: a magnetic reconance study with pulmonary arterial hypertension. Am Heart J 118:990-999, 1989.
2. Naiki T, Takmura S, Matsumoto, T, Hayashi K. Three-dimensional laser Doppler anemometry of pulsatile flow in the models of aortic bifurcation. Med Biol Engr Comp 29:689, 1991.
3. Hatle L, Angelsen. Doppler Ultrasound in Cardiology: Physical Principles and Clinical Applications.. Lea & Febiger, Philadelphia, 1985, p. 90-93.
4. Reller MD, McDonald RW, Gerlis LM, Thornburg KL. Cardiac embryology: basic review and clinical correlations. J Am Soc Echocardiogr 4:519-532, 1991.
5. Hoffman JIE. Incidence. *In* Anderson RH, Macartney FJ, Shinebourne EA, Tynan M (eds), Pediatric Cardiology, Vol 1. London: Churchill Livingstone, 1987, p 4.
6. Blalock A, Taussig HB. Surgical treatment of malformations of the heart in which there is pulmonary stenosis or pulmonary atresia. JAMA 128:189, 1945.
7. Potts WJ. Aortic-pulmonary anastomosis for pulmonary stenosis. J Thorac Surg 17:223, 1948.
8. Edwards WD. Congenital heart disease. *In* Schoen FJ (ed), Interventional and Surgical Cardiovascular Pathology: Clinical Correlations and Basic Principles. Philadelphia: WB Saunders, 1989, pp 281-368.
9. Rastelli GC, Dugley PA, Davis GD, Kirklin JW. Surgical repair for pulmonary valve atresia with coronary-pulmonary artery fistula: report of a case. Mayo Clin Proc 40:521-527, 1965.
10. Ross DN, Somerville J. Correction of pulmonary atresia with a homograft aortic valve. Lancet 2:1446-1447, 1966.
11. Fontan F, Baudet E. Surgical repair of tricuspid atresia. Thorax 26:240-248, 1971.
12. Agarwal KC, Edwards WD, Feldt RH, Danielson GK, Puga FJ, McGoon DC. Clinicopathological correlates of obstructed right-sided porcine-valved extracardiac conduits. J Thorac Cardiovasc Surg 81:591-601, 1981.
13. Pearl J, Haas G, Laks H, Drinkwater D. Management of complications of extracardiac conduits. *In* Waldhausen JA, Orringer MB (eds), Complications in Cardiothoracic Surgery. St. Louis: Mosby, 1991, pp 212-223.
14. Bailey WW, Kirklin JW, Bargeron LM Jr, et al. Late results with synthetic valved external conduits from venous ventricle to pulmonary arteries. Circulation 56:Suppl 2:73, 1977.
15. Ciaravella JM Jr, McGoon DC, Danielson GK, et al. Experience with the extracardiac conduit. J Thorac Cardiovasc Surg 78:920-930, 1979.
16. Ben-Schachar G, Nicoloff DM, Edwards JE. Separation of neointima from Dacron graft causing obstruction: case following Fontan procedure for tricuspid atresia. J Thorac Cardiovasc Surg 82:268-271, 1981.
17. Agarwal KC, Edwards WD, Feldt RH, Danielson GK, Puga FJ, McGoon DC. Pathogenesis of nonobstructive fibrous peels in right-sided porcine-valved extracardiac conduits. J Thorac Cardiovasc Surg 83:584-589, 1982.
18. McGoon DC. Long-term effects of prosthetic materials. *In* Engle ME, Perloff JK (eds). Congenital Heart Disease after Surgery: Benefits, Residua, Sequelae. New York: Yorke Medical Books, 1983, pp 177-201.

19. Schoen FJ. Pathologic analysis of the cardiovascular system and prosthetic devices. Interventional and Surgical Cardiovascular Pathology: Clinical Correlations and Basic Principles. Philadelphia: WB Saunders, 1989, pp 369-396.

20. Fiore AC, Peigh PS, Robison RJ, Glant MD, King H, Brown JW. Valved and nonvalved right ventricular-pulmonary arterial extracardiac conduits: an experimental comparison. J Thorac Cardiovasc Surg 86:490-497, 1983.

21. deLeval MR, Kilner P, Gewillig M, Bull C. Total cavopulmonary connection: a logical alternative to atriopulmonary connection for complex Fontan operations. J Thorac Cardiovasc Surg 96:682-695, 1988.

22. Brown JW, Myerowitz PD, Cann MS, McIntosh CL, Morrow AG. Apical-aortic anastomosis: a method for relief of diffuse left ventricular outflow obstruction. Surg Forum 25:147-149, 1974.

23. Schoen FJ. Vascular disease. Interventional and Surgical Cardiovascular Pathology: Clinical Correlations and Basic Principles. Philadelphia: WB Saunders, 1989, pp 241-280.

24. Brown JW, Halpin MP, Rescorla FJ, VanNatta, Fiore AC, Shipley GD, Bizuneh M, Bills R, Waller B. Externally stented polytetrafluoroethylene valved conduits for right heart reconstruction. J Thorac Cardiovasc Surg 90:833-841, 1985.

25. Glotzer P, Hurwitt. Experimental infundibular bypass. J Thorac Cardiovasc Surg 234-238, 1960.

26. Lucas CL, Henry GW, Ferreiro JI, Ha B, Keagy BA, Wilcox BR. Pulmonary blood velocity profile variability in open-chest dogs: 1) influence of acutely altered hemodynamic states on profiles and 2) influence of profiles on the accuracy of techniques for cardiac output determination. Heart & Vessels 4:65-78, 1988.

27. Lucas CL, Henry GW, Ha B, Ferreiro JI, Frantz EG, Wilcox BR. Characterization of pulmonary artery blood velocity patterns in lambs. *In* Liepsch DW (ed), Biofluid Mechanics: Blood Flow in Large Vessels. Springer-Verlag, 1990 pp. 171-184.

28. Lynch PG, Yoganathan AP, Ha B, Henry GW, Lucas CL. The effects of curvature on fluid flow fields in pulmonary artery models: flow visualization studies. JBiomech Engr (in press).

29. Carroll SL, Katayama H, Henry GW, Ferreiro J, Zalesak R, Ha B, Lucas CL, Singh M, Ha B, Lynch PG, Yoganathan AP. Flow visualization in anatomically accurate, flow-through models of the main pulmonary artery. Cardiol Young 2:114-120, 1992.

30. Freedom RM, Culhan G, Silver MM. Postopertive congenital cardiac disease: selected topics with emphasis on morphological aberations and correlated angiocardiography. *In* Silver MD (ed), Cardiovascular Pathology. New York: Churchill Livingstone 1983, pp 1225-1295.

31. Matsumoto H, Miyawaki F, Takayama T, Asaano K. Wrapped-knitted dacron and microporous EPTFE conduits for reconstruction of right ventricular outflow tract. Jap J Surg 15:249-253, 1985.

32. Fiore AC, Peigh PS, Sears NJ, Deschner WP, Brown JW. The prevention of extra cardiac conduit obstruction: an experimental study. J Surg Res 34:463-472, 1983.

33. Gilbert JW, Cornell WP, Cooper T. An experimental study of pulmonary artery replacement. J Thorac Cardiovasc Surg 667-672, 1960.

34. Fiore AC, Brown JW, Cromartie RS, Ofstein LC, Peigh PS, Sears NS, Deschner WP, King H. Prosthetic replacement for the thoracic vena cava. J Thorac Cardiovasc Surg 84:560-568, 1982.

35. Chandran KB, Yearwood TL, Wieting DW. An experimental study of pulsatile flow in a curved tube. J Biomech 12:793-805, 1979.

36. Yearwood TL, Chandran KB. Physiological pulsatile flow experiments in a model of the human aortic arch. J Biomech 15:683-704, 1984.

37. Talukder N, Nerem RM. Flow characteristics in vascular graft models. 1st International Conference on Mechanics in Medicine and Biology, Aachen, 1978, pp 181-184.

38. Walburn FJ, Stein PD. Velocity profiles in symmetrically branched tubes simulating the aortic bifurcation. J Biomech 14:601-611, 1981.

39. Bharadvaj BK, Mabon RF, Giddens DP. Steady flow in a model of the human carotid bifurcation. Part I: Flow visualization. J Biomech 15:349-362, 1982.

40. Batten JR, Nerem RM. Model study of flow in curved and planar arterial bifurcations. Cardiovasc Res 16:178-186, 1982.

41. Bharadvaj BK, Mabon RF, Giddens DP. Steady flow in a model of the human carotid bifurcation. Part II: Laser-Doppler anemometer measurements. J Biomech 15:363-373, 1982.

42. Ku DN. Hemodynamics and atherogenesis at the human carotid bifurcation. Ph.D. Thesis, Georgia Institute of Technology, Atlanta, GA, 1983.

43. Friedman MH, Hutchins GM, Bargeron CB, Deters OJ, Mark FF. Correlation of human arterial morphology with hemodynamic measurements in arterial casts. J Biomech Eng 103:204-207, 1981.

44. Karino T, Motomiya M. Flow visualization in isolated transparent natural blood vessels. Biorheology 20:119-127, 1983.

45. Mark FF, Bargeron CB, Deters OJ, Friendman MH. Variations in geometry and shear rate distribution in casts of human aortic bifurcations. J. Biomechanics 22:577-582, 1989.

46. Ku DN, Giddens DP, Zarins CK, Glagov S. Pulsatile flow and atherosclerosis in the human carotid bifurcation: positive correlation between plaque location and low and oscillating shear stress. Arteriosclerosis 5:293-302, 1985.

47. Friedman MH, Deters OJ, Bargeron CB, Hutchins GM, Mark FF. Shear-dependent thickening of the human arterial intima. Atherosclerosis 60:161-171, 1986.

48. Friedman MH, Hutchins GM, Bargeron CB, Deters OJ, Mark FF, Correlation between wall shear and intimal thickness a coronay artery branch. Atherosclerosis 68:27-33, 1987.

49. Friedman MH, Deters OJ, Mark FF, Bargeron CB, Hutchins GM. Arterial geometry affects hemodynamics. Atherosclerosis 46:225-231, 1983.

50. Bargeron CB, Hutchins GM, Moore GW, Deters OJ, Mark FF, Friedman MH. Distribution of the geometric parameters of human aortic bifurcations. Arteriosclerosis 6:109-113, 1986.

51. Sung HW, Yoganathan AP. Secondary flow velocity pattern in a pulmonary artery model with varying degrees of valvular pulmonic stenosis: pulsatile *in vitro* studies. J Biomech Eng 12:88-92, 1990.

52. Sung HW, Yoganathan AP. Axial flow velocity pattern in a pulmonary artery model with varying degrees of valvular pulmonic stenosis: pulsatile *in vitro* studies. J Biomech 23:565-578, 1990.

53. Yoganathan AP, Valdes-Cruz LM, Schmidt-Dohna J, Jimoh A, Berry C, Tamura T, Sahn DJ. Continuous-wave Doppler velocities and gradients across fixed tunnel obstructions: studies in vitro and in vivo. Cirulation 76:657-666, 1987.

54. Philpot E, Yoganathan AP, Sung HW, Woo YR, Franch RH, Sahn DJ, Valdez-Cruz L. In-vitro pulsatile flow visualization studies in a pulmonary artery model. Transac ASME 107:368-375, 1985.

55. Yoganathan AP, Ball J, Woo YR, Philpot EF, Sung HW. Steady flow velocity measurements in a pulmonary artery model with varying degrees of pulmonic stenosis. J Biomech 19:129-146, 1986 .

56. Woo YR, Yoganathan AP. Two-component laser Doppler anemometer for measurement of velocity and turbulent shear stress near prosthetic heart valves. Med Instrumentation 19:224-231, 1985.

57. Jones M, McMillan ST, Eidbo EE, Woo Y-R, Yoganathan AP. Evaluation of prosthetic heart valves by Doppler flow imaging. Echocardiography 3:513-525, 1986.

58. Laschinger JC, Vannier MW, Gronemeyer S, Gutierrez F, Rosenbloom M, Cox JL. Noninvasive three-dimensional reconstruction of the heart and great vessels by ECG-gated magnetic resonanace imaging: a new diagnostic modality. Annals of Thoracic Surgery 45:505-514, 1988

59. Laschinger JC, Vannier MW, Guitierrez F, Gronemeyer S, Weldon CS, Spray TL, Cox JL. Preoperative three-dimensional reconstruction of the heart and great vessels in patients with congenital heart disease. J. of Thoracic and Cardiovascular Surgery 96:464-473, 1988.

60. Edwards FH, Wind G, Thompson LeN, Bellamy RF, Barry MJ, Schaefer PS. Three-dimensional image reconstruction for planning of a complex cardiovascular procedure. Annals of Thoracic Surgery 49:486-488, 1990.

61. Brewster LJ, Trivedi SS, Tuy HK, Udupa JK. Interactive surgical planning. IEEE Computer Graphics Applic 4:31-40, 1984.

62. Liu Y-H, Mair DD, Hagler DJ, Seward JB, Julsrud Pr, Ritman EL. Angiography for delineation of systemic-to-pulmonary shunts in congenital pulmonary atresia: evaluation with the dynamic spation reconstructor. May Clin Proc 61:932-941, 1986.

63. Ha B, Lucas CL, Henry GW, Yoganathan AP, Ferreiro JI, Wilcox BR. Two-dimensional pulmonary artery velocity profiles in growing lambs. Proc 12th Annual Conf IEEE, Inc 12:519-520, 1990.

64. Ha B, Katayama H, Krzeski R, Lucas CL, Henry GW, Lynch P, Yoganathan AP, Ferreiro JI, Wilcox BR. Pulmonary artery velocity profiles in young lambs. Proc of 9th Engineering Mechanics Conf. LD Lutes, JM Niedzwecki (eds). Am Soc of Civil Engineers, New York, 836-839, 1992.

65. Carroll SL, Henry GW, Katayama H, Zalesak R, Ferreiro J, Lucas CL, Singh M, Ha B, Lynch PG, Yoganathan AP. Flow visualization in anatomically accurate, flow-through models of the main pulmonary artery trunk. *In* Swamy NVC, Singh M (eds), Physiological Fluid Dynamics III. Narosa Publishing House, 1992, pp 44-49.

66. Katayama H, Carroll S, Zalesak R, Ha B, Lucas C, Ferreiro J, Henry W, Singh M. An anatomically accurate flow-through model of the pulmonary vasculature. Med Biol Engr Comp 29:247, 1991.

67. Friedman MH, Bargeron CG, Hutchins GM, et al. Hemodynamic measurements in human arterial casts, and their correlation with histology and luminal area. J Biomech Eng 102:247-251, 1980.

68. Duncan DD, Bargeron CB, Friedman MH. The effect of compliance on wall shear in casts of the human aortic bifurcation. J Biomech Eng 112:183-188, 1990.

69. Liepsch D, Baumgart R. Laser-Doppler-velocity measurements in a true-to-scale elastic model of the human aortic arch. A I King *In* SA Lantz (ed), Advances in Bioengineering. ASME, Bed-Vol 12, 1986, pp 150-151.

70. Liepsch D, Moravec S. Pulsatile flow of non-Newtonian fluid in distensible models of human arteries. Biorheology 21:571-586, 1984.

71. Anayiotos A. Fluid dynamics at a compliant bifurcation model. Ph.D. Thesis, Georgia Institute of Technology, 1990.

72. Wells MK, Histand MB, Reeves JT, et al. Ultrasonic transesophageal measurement of hemodynamic parameters in humans. ISA Transac 18:57-61, 1979.

73. Lucas CL, Henry GW, Frantz E, Ha B, Ferreiro JI, Wilcox BR. The role of maturation in pulmonary vascular dynamics. *In* Schneck DJ, Lucas CL (eds), Biofluid Mechanics III New York: New York University Press, 1990, pp 23-32.

74. Lucas CL, Wilcox BR, Henry GW, Ferreiro JI, Singh M. Influence of posture variation on fluid flow patterns in a curved tube. Biorheology 27:797-805, 1990.

75. Singh M, Lucas CL, Henry GW, Ferreiro JI, Wilcox BR. Multiangle visualization of flow patterns in saccular aneurysms. Biorheology 28:333-339, 1991.

76. Singh M, Lucas CL, Henry GW, Ferreiro JI, Wilcox BR. Multiangle visualization of flow patterns in arterial bifurcation models. Biorheology 27:969-970, 1990.

77. Zhao C, Ha B, Henry GW, Ferreiro JI, Lucas C, Wilcox BR. Computation of three-dimensional geometric features for pulmonary artery bifurcation. FASEB, Atlanta, April 1991.

78. Zhao C, Ha B, Katayama H, Krzeski R, Henry G, Ferreiro J, Lucas C, Wilcox B. Evaluation of the maturation of pulmonary artery geometry. FASEB J 6:A2045, 1992.

79. Peskin CS, McQueen DM. A three-dimensional computational method for blood flow in the heart. I. Immersed elastic fibers in a viscous incompressible fluid. J. of Computational Physics, 81(2)372-405, 1989.

80. Hartley, CJ. Three channel ultrasonic mainframe, S/N 0751, Operations manual. Instrumentation Development Laboratories, Baylor College of Medicine, 1989.

81. Lucas CL, Keagy BA, Hsiao HS, Wilcox BR. Software analysis of 20 MHz pulsed Doppler quadrature data. Ultrasound Med Biol 9:641–655, 1983.

82. Lucas CL, Henry GW, Criado E, Ferreiro JI, Baudino M, Keagy BA, Wilcox BR. Frequency response: zerocrosser versus first moment average. Proc 38th Annual Conf Eng Med Biol 27:159, 1985.

83. Hartley CJ, Hanley HG, Lewis RM, Cole JS. Synchronized pulsed Doppler blood flow and ultrasonic dimension measurement in conscious dogs. Ultrasound Med Biol 4:99-110, 1978.

84. Cole JS, Hartley CJ. The pulsed Doppler coronary artery catheter: preliminary report of a new technique for measuring rapid changes in coronary artery flow velocity in man. Circulation 56:18–25, 1977.

85. Driscoll DJ, Gillete PC, Lewis RM, Driscoll DJ, Gillette PC, Lewis RM, Hartley CJ, Schwartz A. Comparative hemodynamic effects of isoproterenol, dopamine and dobutamine in the newborn dog. Pediatr Res 13:1006–1009, 1979.

86. Ha B, Lucas CL, Henry GW, Ferreiro JI, Keagy BA, Wilcox BR. Comparison of two pulsed Doppler techniques for measuring pulmonary velocity profile. Proc 13th Northeast Bioeng Conf IEEE, Inc., 2:361-364, 1987.

87. Henry GW, Lucas CL, Keagy BA, Criado E, Ferreiro JI, and Wilcox BR. The effect of left to right shunting on the velocity profile in the pulmonary artery in a canine model. Ultrasound Med Biol 11(Suppl):386, 1985.

88. Michler RE, Rose EA, Malm JR. Tricuspid atresia. *In* Arciniegas E (ed), Pediatric Cardiac Surgery. Chicago: Year Book Medical Publishers, 1985, pp 297-313.

89. Marcelletti C, Corno A, Giannico S, Marino B. Inferior vena-cava-pulmonary artery extracardiac conduit. J Thorac Cardiovasc Surg 100:228-232, 1990.

90. Lucas CL, Wilcox BR, Ha B, Henry GW. Comparison of time domain algorithms for estimating aortic characteristic impedance in humans. IEEE Trans Biomed Eng 35:62-68, 1988.

91. Katayama H, Henry GW, Lucas CL, Ha B, Ferreiro JI, Frantz EG, Krzeski R. Three-dimensional visualization of pulmonary blood flow velocity profiles in lambs. Japanese Heart J 33:95-111, 1992.

92. Greenwald SE, Johnson RJ, Haworth SG. Pulmonary vascular input impedance in the newborn and infant pig. Cardiovasc Res 18:44-50, 1985.

93. Melbin J, Brown DJ, Noordergraaf A. Pulmonary blood flow and large vessel function. Proc 4th AVMF, 40-46, 1986.

94. Melbin J, Brown D, Li K-J J, Noordergraaf A. Non linear systems limitations of models and measurements. Proc 7th Internat Conf Workshop Cardiovasc System Dynamics Soc, Zuoz, Switzerland, 1986.

95. Grant JB, Pardowski LJ, Fitzpatrick JM. Effect of perivascular electromagnetic flow probes on pulmonary hemodynamics. J Appl Physiol 65:1885-1890.

96. Burton RG, Gorewit RC. Ultrasonic flowmeter uses wide-beam transit-time technique. Med Electronics 15:68-73, 1984.

97. Franch RH, Gay BB. Congenital stenosis of the pulmonary artery branches. Am J Med 35:512-529, 1963.

98. Fung YC. Biomechanics: Motion, Flow, Stress, and Growth. Springer-Verlag, New York, 1990.

99. Gunzburger MD. Finite Element Methods for Viscous Incompressible Flows. Academic Press, Boston, 1989.

100. Reuderink, PJ. Analysis of the flow in a 3D distensible model of the carotid artery bifurcation. PhD Thesis, Eindhoven University, 1991.

101. Perry AE, Chong MS. A description of eddying motions and flow patterns using critical point concepts. Annual Review of Fluid Mechanics 19:125-155, 1987.

102. Hesselink L. Digital image processing in flow visualization. Annual Review of Fluid Mechanics 20:421-486, 1988.

103. Helman JL, Hesselink L. Analysis and visualization of flow topology in numerical data sets. In Moffatt HK and Tsinober A (eds). Topological Fluid Mechanics. Cambridge University Press, Cambridge (UK), 1990, pp. 361-371.

104. Bakker PG, Winkel MEM. On the topology of three-dimensional separated flow structures and local solutions of the Navier-Stokes Equations. In Moffatt HK and Tsinober A (eds). Topological Fluid Mechanics. Cambridge University Press, Cambridge (UK), 1990, pp. 384-394.